Gating and Ionic Currents Reveal How the BK_{Ca} Channel's Ca^{2+} Sensitivity Is Enhanced by its β1 Subunit

Lin Bao and Daniel H. Cox

Molecular Cardiology Research Institute, New England Medical Center, and Department of Neuroscience, Tufts University School of Medicine, Boston, MA 02111

Large-conductance Ca^{2+}-activated K^+ channels (BK_{Ca} channels) are regulated by the tissue-specific expression of auxiliary β subunits. β1 is predominately expressed in smooth muscle, where it greatly enhances the BK_{Ca} channel's Ca^{2+} sensitivity, an effect that is required for proper regulation of smooth muscle tone. Here, using gating current recordings, macroscopic ionic current recordings, and unitary ionic current recordings at very low open probabilities, we have investigated the mechanism that underlies this effect. Our results may be summarized as follows. The β1 subunit has little or no effect on the equilibrium constant of the conformational change by which the BK_{Ca} channel opens, and it does not affect the gating charge on the channel's voltage sensors, but it does stabilize voltage sensor activation, both when the channel is open and when it is closed, such that voltage sensor activation occurs at more negative voltages with β1 present. Furthermore, β1 stabilizes the active voltage sensor more when the channel is closed than when it is open, and this reduces the factor *D* by which voltage sensor activation promotes opening by ~24% (16.8→12.8). The effects of β1 on voltage sensing enhance the BK_{Ca} channel's Ca^{2+} sensitivity by decreasing at most voltages the work that Ca^{2+} binding must do to open the channel. In addition, however, in order to fully account for the increase in efficacy and apparent Ca^{2+} affinity brought about by β1 at negative voltages, our studies suggest that β1 also decreases the true Ca^{2+} affinity of the closed channel, increasing its Ca^{2+} dissociation constant from ~3.7 μM to between 4.7 and 7.1 μM, depending on how many binding sites are affected.

The Journal of General Physiology

INTRODUCTION

Auxiliary subunits often tune ion channel behavior to the needs of a particular cell type (Isom et al., 1994; Gurnett and Campbell, 1996; Xu et al., 1998). This method of generating functional diversity is particularly well exploited by the large-conductance Ca^{2+}-activated potassium channel, or BK_{Ca} channel, which is composed of pore-forming α and auxiliary β subunits (Knaus et al., 1994b; McManus et al., 1995). Four α subunits are sufficient to form a fully functional channel complete with Ca^{2+} sensitivity, voltage sensitivity, and a large single-channel conductance (Shen et al., 1994; DiChiara and Reinhart, 1995; Cui et al., 1997). There is only a single gene for this subunit (Atkinson et al., 1991; Adelman et al., 1992; Butler et al., 1993). In different tissues, however, BK_{Ca} channels display different phenotypes, and this is thought to be due primarily to the tissue-specific expression of some subset of four homologous BK_{Ca} β subunits (β1–β4) (Knaus et al., 1994a; McManus et al., 1995; Wallner et al., 1995, 1999; Meera et al., 1996, 2000; Tanaka et al., 1997; Xia et al., 1999, 2000; Behrens et al., 2000; Brenner et al., 2000a; Uebele et al., 2000; Weiger et al., 2000).

The β2 subunit, for example, confers rapid inactivation upon the BK_{Ca} channels of adrenal chromaffin cells (Wallner et al., 1999; Xia et al., 1999), and β4 renders many of the BK_{Ca} channels of the brain insensitive to the scorpion toxin charybdotoxin (Meera et al., 2000). Perhaps most profound, however, the BK_{Ca} β1 subunit, which is predominately expressed in smooth muscle, slows the BK_{Ca} channel's kinetic behavior and dramatically increases its Ca^{2+} sensitivity (McManus et al., 1995; Wallner et al., 1995; Meera et al., 1996; Cox and Aldrich, 2000; Nimigean and Magleby, 2000). In fact, mice that lack β1 have hypertension, because the BK_{Ca} channels of their vascular smooth muscle lack the Ca^{2+} sensitivity required for BK_{Ca}-mediated feedback regulation of smooth muscle contraction (Brenner et al., 2000b). Thus, β1 is important in the vascular system and indeed in many other smooth muscle–dependent systems as well (Nelson and Quayle, 1995; Snetkov and Ward, 1999; Bayguinov et al., 2001; Niu and Magleby, 2002; Meredith et al., 2004; Morales et al., 2004). Four β1 subunits associate with a single BK_{Ca} channel (Wang et al., 2002).

How β1 enhances the BK_{Ca} channel's Ca^{2+} sensitivity is not well understood. Perhaps the simplest mechanism would be for it to increase the affinities of the channel's Ca^{2+}-binding sites, but this does not appear to be the case. Nimigean and Magleby (1999, 2000) found that

Correspondence to Daniel H. Cox: dan.cox@tufts.edu

Abbreviation used in this paper: BK_{Ca}, large-conductance Ca^{2+}-activated K^+ channel.

β1 increases the length of time that the BK_{Ca} channel spends in bursting states and that this effect persists in the absence of Ca^{2+}. They suggested that it is this Ca^{2+}-independent effect that underlies most of the channel's increased Ca^{2+} sensitivity. Furthermore, we found previously that as the Ca^{2+} concentration is raised, the concentration at which the BK_{Ca} channel's conductance–voltage relation begins to shift leftward is essentially unaffected by β1 (Cox and Aldrich, 2000), a result that suggests that, at least when it is open, the channel's affinity for Ca^{2+} is not greatly altered by β1. In fact, this study leads us to suggest that, rather than greatly altering the channel's Ca^{2+}-binding properties, β1 may be enhancing its voltage-sensing properties by shifting the equilibrium for voltage sensor activation, and therefore the channel's gating charge vs. voltage relation (Q–V relation) ~100 mV toward more negative voltages. This would be expected to decrease the work that Ca^{2+} binding must do to open the channel at most voltages and thereby bring about an apparent increase in Ca^{2+} affinity at most voltages as well. Contrary to this hypothesis, however, Orio and Latorre (2005) have recently proposed that it is a decrease in effective gating charge, rather that a shift in the channel's Q–V relation, that accounts for the effects of β1.

Here, to distinguish between these possibilities, we have measured gating currents from heterologously expressed BK_{Ca} channels with and without β1 coexpression. Our results indicate that the channel's Q–V relation does shift dramatically leftward upon β1 coexpression, with no change in gating charge. Thus, β1 stabilizes the active conformation of the channel's voltage sensors, and this has a large effect on the Ca^{2+} sensitivity of the channel. In addition, however, in order to fully account for the increase in apparent Ca^{2+} affinity brought about by β1, we have also found it necessary to suppose that β1 decreases the true affinity of the closed channel for Ca^{2+}.

MATERIALS AND METHODS

Channel Expression

Experiments were done with a BK_{Ca} channel α subunit clone from mouse mSlo-mbr5 (Butler et al., 1993) and a β1 subunit clone from bovine (bβ1) (Knaus et al., 1994a). In vitro transcription was performed with the mMessage mMachine kit with T3 or T7 RNA polymerase (Ambion). 0.05–250 ng of total cRNA was injected into *Xenopus laevis* oocytes 2–6 d before recording. Different amounts of cRNA were injected for different purposes, 0.05–0.2 ng for single channel recording, 10–50 ng for macroscopic current recording, and 150–250 ng for gating currents and limiting P_{open} recordings. bβ1 and mSlo cRNA were mixed in a molar ratio of 2:1 before injection.

Electrophysiology

All recording were done in the inside-out patch clamp configuration (Hamill et al., 1981). Patch pipettes were made of borosilicate glass (VWR micropipettes) with 0.5–4 MΩ resistances that were varied for different recording purposes. The tips of the patch pipettes were coated with sticky wax (Sticky Wax) and fire polished. Data were acquired using an Axopatch 200B patch-clamp amplifier and a Macintosh-based computer system equipped with an ITC-16 hardware interface (Instrutech) and Pulse acquisition software (HEKA Electronik). For macroscopic current recording, data were sampled at 50 kHz and filtered at 10 kHz.

In most macroscopic current experiments, capacity and leak currents were subtracted using a P/5 subtraction protocol with a holding potential of −120 mV and leak pulses opposite in polarity to the test pulse, but with $BK_{\alpha+\beta1}$ currents recorded at 10 and 100 μM Ca^{2+} no leak subtraction was performed.

Unitary currents were sampled at 100 kHz and filtered at 10 kHz. For gating current recordings, voltage commands were filtered at 7.5 kHz to limit the size of fast capacity transients, and the data were sampled at 100 kHz and filtered at 5–10 kHz. Capacity and leak currents were subtracted using a P/5 protocol with a holding potential of −120 mV and leak pulses opposite in polarity to the test pulse. All experiments were performed at room temperature, 22–24°C.

Solutions

Gating current solutions were made according to Horrigan and Aldrich (1999). Pipette solutions contained (in mM) 127 TEA-OH, 125 $HMeSO_3$, 2 HCl, 2 $MgCl_2$, 20 HEPES, pH 7.2 (adjusted with $HMeSO_3$ or TEA-OH). The 0.5 nM Ca^{2+} internal solution contained (in mM) 141 NMDG, 135 $HMeSO_3$, 6 HCl, 20 HEPES, 40 μM (+)-18-crown-6-tetracarboxylic acid (18C6TA), 5 EGTA, pH 7.2 (adjusted with NMDG and $HMeSO_3$).

K^+ current recording solutions were composed of the following (in mM): pipette solution, 80 KOH, 60 NMDG, 140 $HMeSO_3$, 20 HEPES, 2 KCl, 2 $MgCl_2$ (pH 7.20); internal solution, 80 KOH, 60 NMDG, 140 $HMeSO_3$, 20 HEPES, 2 KCl, 1 HEDTA or 1 EGTA, and $CaCl_2$ sufficient to give the appropriate free Ca^{2+} concentration (pH 7.20). EGTA (Sigma-Aldrich) was used as the Ca^{2+} buffer for solutions containing <1 μM free [Ca^{2+}]. HEDTA (Sigma-Aldrich) was used as the Ca^{2+} buffer for solutions containing between 1 and 10 μM free Ca^{2+}, and no Ca^{2+} chelator was used in solutions containing 100 μM free Ca^{2+}. 50 μM (+)-18-crown-6-tetracarboxylic acid (18C6TA) was added to all internal solutions to prevent Ba^{2+} block at high voltages (Cox et al., 1997b).

The appropriate amount of total Ca^{2+} (100 mM $CaCl_2$ standard solution; Orion Research Inc.) to add to the base internal solution containing 1 mM HEDTA to yield the desired free Ca^{2+} concentration was calculated using the program Max Chelator (http://www.stanford.edu/~cpatton/maxc.html), and the solutions were prepared as previously described (Bao et al., 2004). To change Ca^{2+} concentration, the solution bathing the cytoplasmic face of the patch was exchanged using a sewer pipe flow system (DAD 12) purchased from Adams and List Assoc. Ltd.

Data Analysis

All data analysis was performed with Igor Pro graphing and curve fitting software (WaveMetrics Inc.), and the Levenberg-Marquardt algorithm was used to perform nonlinear least-squares curve fitting. Values in the text are given ± SEM.

G–V Curves. Conductance–voltage (G–V) relations were determined from the amplitude of tail currents measured 200 μs after repolarizations to −80 mV following voltage steps to the test voltage. Each G–V relation was fitted with a Boltzmann function

$$G = \frac{G_{max}}{1 + e^{-zF(V - V_{1/2})/RT}} \quad (1)$$

and normalized to the maximum of the fit. The half-activation voltage ($V_{1/2}$) and the effective gating charge (z) were determined from the fitting.

Q–V Curves. The amount of activated gating charge (Q) at a given voltage was determined from the area under the gating current trace between 0 and 300 μs after the initiation of the voltage step. Repolarizations were to −80 mV. Each Q–V relation was fitted with a Boltzmann function and normalized to the maximum of the fit. The voltage sensor's half-activation voltage V_{hc} and the gating charge z_J were determined from the fitting.

Limiting P_{open} Analysis. P_{open} measurements $<10^{-3}$ were made in 3 nM Ca^{2+} with patches that contained hundreds of channels. The number of channels in a given patch (N) was determined by switching the patch into a solution that contained either 100 μM Ca^{2+} (α) or 10 μM Ca^{2+} (α+β1) and recording macroscopic currents at moderate to high voltages. $N$was than calculated as $N = I/(iP_O)$, where i represents the single channel current at a given voltage and P_O represents the open probability at that same voltage. Both i and P_O were determined previously in separate experiments. In some experiments P_O was estimated from the G–V relation determined from the same patch. After determining the number of channels in a given patch, the membrane voltage was moved to lower voltages, the patch was superfused with a 3 nM Ca^{2+} solution, and unitary currents were recorded for 5–30 s at progressively more negative voltages. All-points histograms were then used to determine the probability of observing 0, 1, 2, 3, ... open channels at a given time, and true channel P_{open} was then determined as

$$P_{open} = \frac{1(Ft_{open\_1}) + 2(Ft_{open\_2}) + 3(Ft_{open\_3}) + \ldots n(Ft_{open\_n}) + \ldots N(Ft_{open\_N})}{N}, \quad (2)$$

where Ft_{open_n} represents the fraction of time n channels are open during the recording.

Fitting τ–V Curves Based on the Model of Horrigan et al. (1999). Relaxation time constants as a function of voltage were calculated for Scheme I (see Fig. 5) assuming its horizontal steps equilibrate much more rapidly than its vertical steps, such that they are always at equilibrium (Cox et al., 1997a; Cui et al., 1997; Horrigan et al., 1999; Horrigan and Aldrich, 2002). Under this assumption, τ(V) can be calculated as a weighted average of all the vertical rate constant in Scheme I as follows:

$$\delta = (\delta_0 \cdot f_{C0} + \delta_1 \cdot f_{C1} + \delta_2 \cdot f_{C2} + \delta_3 \cdot f_{C3} + \delta_4 \cdot f_{C4})$$

$$\gamma = (\gamma_0 \cdot f_{O0} + \gamma_1 \cdot f_{O1} + \gamma_2 \cdot f_{O2} + \gamma_3 \cdot f_{O3} + \gamma_4 \cdot f_{O4}) \quad (3)$$

$$\tau = \frac{1}{\delta(V) + \gamma(V)},$$

where δ_x and γ_x represent closed-to-open and open-to-closed rate constants, respectively, and f_{cx} and f_{ox} represent the fraction of closed or open channels occupying the state that precedes each transition. These fractions for the closed channel were calculated as follows:

$$Jc = e^{z_J F(V - V_{hc})/RT}$$

$$f_{C0} = 1/(1 + 4Jc + 6Jc^2 + 4Jc^3 + Jc^4)$$

$$f_{C1} = 4Jc/(1 + 4Jc + 6Jc^2 + 4Jc^3 + Jc^4)$$

$$f_{C2} = 6Jc^2/(1 + 4Jc + 6Jc^2 + 4Jc^3 + Jc^4) \quad (4)$$

$$f_{C3} = 4Jc^3/(1 + 4Jc + 6Jc^2 + 4Jc^3 + Jc^4)$$

$$f_{C4} = Jc^4/(1 + 4Jc + 6Jc^2 + 4Jc^3 + Jc^4)$$

For the open channel, f_{O0}–f_{O4} were calculated in the same way but using Jo rather than Jc. Each vertical rate constant was also assigned a voltage dependence as follows

$$\delta_x = \delta_x(0) e^{z_\delta FV/RT} \qquad \gamma_x = \gamma_x(0) e^{z\gamma FV/RT}, \quad (5)$$

where x = (0, 1, 2, 3, 4, 5) and $z_\gamma + z_\delta = z_L$. For a given vertical step, once the forward rate was specified, the backward rate was determined by the equilibrium parameters of the model.

$$\delta_x = L_x \gamma_x \qquad L_x = D^x L e^{z_L FV/RT} \quad (6)$$

Thus, to fit the τ–V curves in Fig. 7, 11 independent parameters were required: L, V_{hc}, D, z_J, z_L, z_γ, $\gamma_0(0)$, $\gamma_1(0)$, $\gamma_2(0)$, $\gamma_3(0)$, and $\gamma_4(0)$. For definitions of L, V_{hc}, D, z_J, and z_L see RESULTS.

RESULTS

Steady-state Effects of β1

The BK_{Ca} channel is both Ca^{2+} and voltage sensitive, and the effects of these stimuli together are often displayed as a series of conductance–voltage (G–V) relations determined over a series of Ca^{2+} concentrations (Barrett et al., 1982). Such a series, determined from currents recorded from channels expressed in *Xenopus* oocyte macropatches is shown in Fig. 1 C. These G–V curves were derived from channels composed of α subunits alone. When the BK_{Ca} β1 subunit is coexpressed with the α subunit, the Ca^{2+}-induced leftward shifting evident in Fig. 1 C becomes more pronounced (Fig. 1, D and E; see also Table I) (McManus et al., 1995; Wallner et al., 1995; Meera et al., 1996; Cox and Aldrich, 2000), and thus it may be said that β1 increases the Ca^{2+} sensitivity of the BK_{Ca} channel in that it increases its G–V shift in response to changes in Ca^{2+} concentration (McManus et al., 1995).

This increase in Ca^{2+} sensitivity can been viewed in a more conventional manner if a single voltage is considered. At −40 mV, for example, β1 dramatically in-

TABLE I

Comparing G–V Parameters

	BK_α			$BK_{\alpha+\beta1}$		
[Ca]	$V_{1/2}$	$Q(e)$	n	$V_{1/2}$	$Q(e)$	n
μM	mV	e		mV	e	
0.003	203 ± 5.3	0.95 ± 0.03	4	215 ± 3.4	0.66 ± 0.03	16
1	125 ± 4.7	1.35 ± 0.12	7	82 ± 3.4	0.99 ± 0.02	20
10	37 ± 5.6	1.26 ± 0.07	8	−60 ± 1.6	1.05 ± 0.05	7
100	1 ± 2.4	1.17 ± 0.03	22	−100 ± 3.5	1 ± 0.06	10

The values shown are Boltzmann-fit parameters. They indicate mean ± SEM.

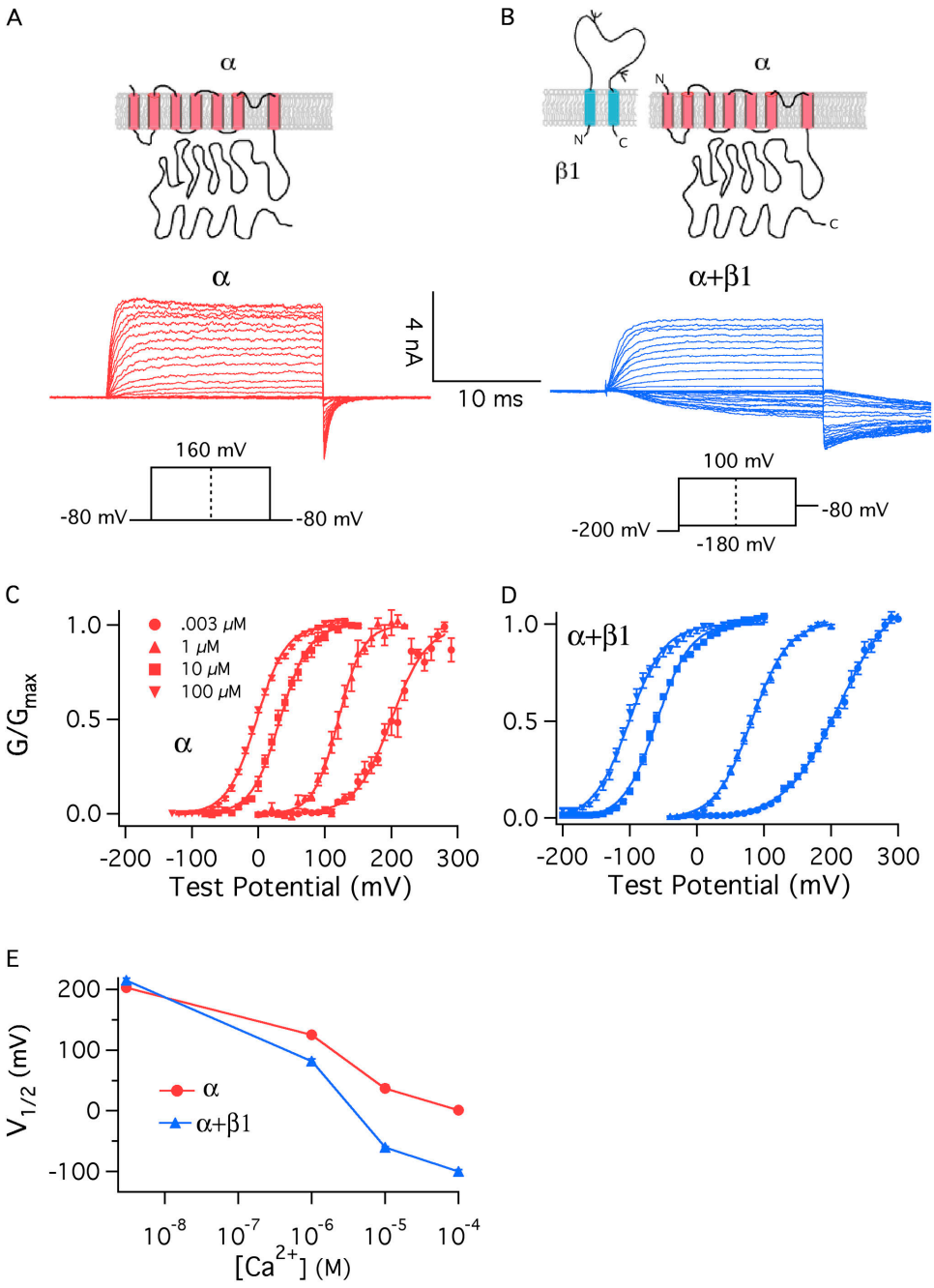

Figure 1. β1 increases the Ca^{2+} sensitivity of the BK_{Ca} channel. (A and B) Macroscopic currents recorded from BK_{α} channels (A) and $BK_{\alpha+\beta1}$ channels (B). Currents are from inside-out *Xenopus* oocyte macropatches exposed to 10 μM internal Ca^{2+}. (C and D) G–V relations determined at the following Ca^{2+} concentrations: 0.003, 1, 10, and 100 μM for the BK_{α} channel (C) and $BK_{\alpha+\beta1}$ channel (D). Each curve represents the average of between 4 and 22 individual curves. Error bars indicate SEM. The solid curves are Boltzmann fits with the following parameters: BK_{α}, 3 nM Ca^{2+}: Q = 0.93 *e*, $V_{1/2}$ = 200.3 mV; 1 μM Ca^{2+}: Q = 1.36 *e*, $V_{1/2}$ = 120.6 mV; 10 μM Ca^{2+}: Q = 1.18 *e*, $V_{1/2}$ = 32.8 mV; 100 μM Ca^{2+}: Q = 1.15 *e*, $V_{1/2}$ = −2.4 mV. $BK_{\alpha+\beta1}$, 3 nM Ca^{2+}: Q = 0.62 *e*, $V_{1/2}$ = 213.1 mV; 1 μM Ca^{2+}: Q = 0.94 *e*, $V_{1/2}$ = 82.1 mV; 10 μM Ca^{2+}: Q = 1.02 *e*, $V_{1/2}$ = −59.5 mV; 100 μM Ca^{2+}: Q = 0.96 *e*, $V_{1/2}$ = −101 mV. (E) Plots of half-maximal activation voltage ($V_{1/2}$) vs. Ca^{2+} concentration. The $V_{1/2}$ values are from Table I. Error bars represent SEM.

creases both the efficacy and apparent affinity of Ca^{2+} in activating the BK_{Ca} channel (Fig. 2 A). Interestingly, however, and perhaps mechanistically telling, β1's effects on Ca^{2+} sensing are not static with respect to voltage, but rather, they diminish as the membrane potential is made more positive (Fig. 2, B and C).

Conversely, if we examine β1's effects at a single Ca^{2+} concentration, 100 μM (Fig. 2 D), we see that β1 powerfully shifts the channel's G–V relation leftward along the voltage axis (∼100 mV), and it reduces its maximum slope (20%). Here too, however, β1's effects are not static with respect to the fixed stimulus. The β1-induced G–V shift decreases as the internal Ca^{2+} concentration is lowered (Fig. 2, E and F). In fact, at nominally 0 Ca^{2+} (3 nM in our experiments), β1 no longer produces a leftward G–V shift, but, instead, it creates a slight rightward G–V shift and a pronounced decline in G–V steepness (Fig. 2 G; Table I) (Cox and Aldrich, 2000; Nimigean and Magleby, 2000).

β1's Effects on BK_{Ca} Gating Currents

What does the β1 subunit do to the normal process of BK_{Ca} channel gating that creates these large and physiologically important effects? Previously, we addressed

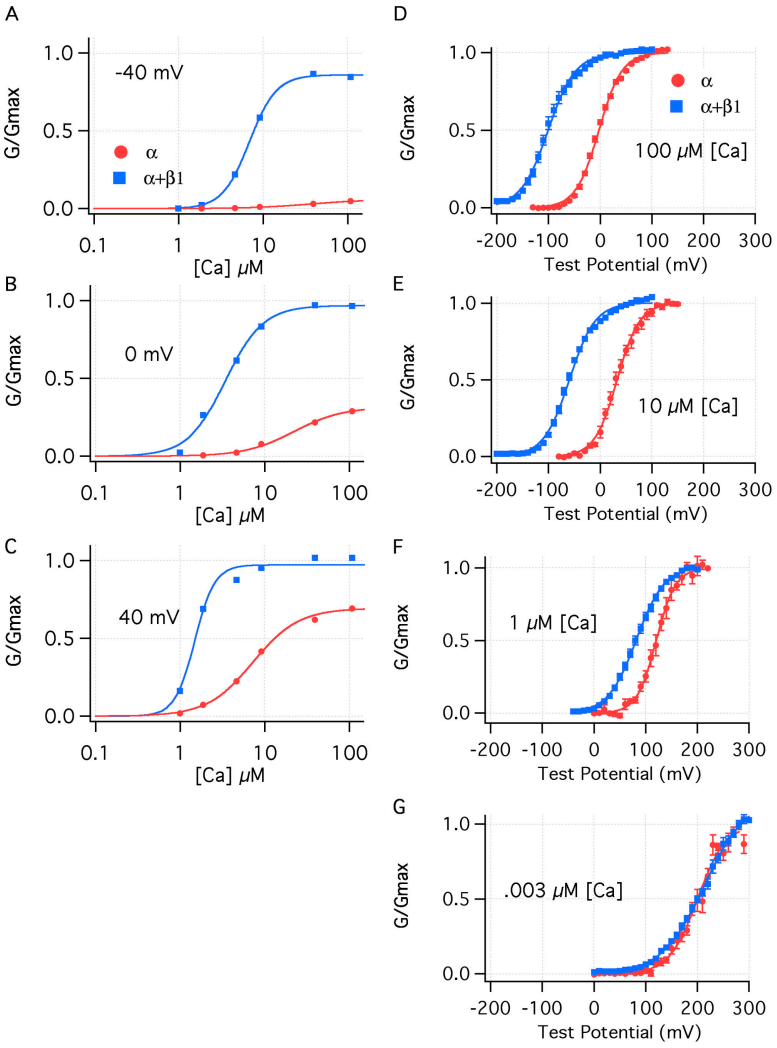

Figure 2. The effects of β1 are both Ca^{2+} and voltage dependent. (A–C) Ca^{2+} dose–response curves determined for the BK_{α} and $BK_{\alpha+\beta1}$ channel at (A) −40, (B) 0, and (C) +40 mV. Curves are fitted with the hill equation:

$$\frac{G}{G_{max}} = \frac{1}{1 + (Kd/[Ca])^{n}}.$$

Fit parameters are as follows: −40 mV, BK_{α} (Kd = 36.5 μM, n = 1.24); $BK_{\alpha+\beta1}$(Kd = 6.89 μM, n = 2.7); 0 mV, BK_{α} (Kd = 22.1 μM, n = 1.5); $BK_{\alpha+\beta1}$ (Kd = 3.4 μM, n = 1.9); +40 mV, BK_{α} (Kd = 7.25 μM, n = 1.6); $BK_{\alpha+\beta1}$(Kd = 3.68 μM, n = 1.5). (D–G) G–V relations are shown for the BK_{α} and the $BK_{\alpha+\beta1}$ channel at (D) 100 μM Ca^{2+}, (E) 10 μM Ca^{2+}, (F) 1 μM Ca^{2+}, and (G) 3 nM Ca^{2+}. The curves are fitted with Boltzmann functions as described in the legend to Fig. 1.

this question by comparing the effects of β1 to what happens to simulated currents when various parameters in models of BK_{Ca} channel gating were altered (Cox and Aldrich, 2000). From this work we concluded that multiple aspects of gating are likely altered by β1, including small changes in Ca^{2+} binding, gating charge, and the intrinsic energetics of channel opening. One large change we predicted, however, was a large β1-induced leftward shift in the channel's charge–voltage (Q–V) relation. This, we supposed, would lower the free energy difference between open and closed states at most voltages, and thus lower as well the work Ca^{2+} binding must do to open the channel (Cox and Aldrich, 2000).

Here, to directly test this prediction we have examined BK_{Ca} gating currents in the absence and presence of β1. A family of gating currents for the BK_{α} channel is shown in Fig. 3 A. These currents were recorded in the essential absence of Ca^{2+} (0.5 nM) with 1-ms voltage steps. Most notable, they are small and fast, 500–1,000 times smaller than the ionic currents we typically observe under the same conditions of channel expression (Fig. 1 A), and at +160 mV (Fig. 3 A, fourth trace down) the ON gating current decays with a time constant of 57.2 ± 4.0 μs (n = 16), and the OFF gating current at −80 mV is similarly fast (τ(off) = 31.2 ± 3.3 μs, n = 20). Thus, care had to be taken to ensure that what we were observing was in fact gating current and not the result of capacity current subtraction errors. We are confident, however, that these currents are in-

TABLE II

Comparing Voltage Gating Parameters

Parameter	BKα (Horrigan et al., 1999)	BK_{α}	$BK_{\alpha+\beta1}$	Difference
L	2×10^{-6}	2.2×10^{-6}	2.5×10^{-6}	0.3×10^{-6}
z_J	0.5 e	0.58 e	0.57 e	0.01
z_L	0.4 e	0.41 e	0.41 e	0
V_{hc}	155 mV	151 mV	80 mV	−71 mV
V_{ho}	24 mV	27 mV	−34 mV	−61 mV
D	17	16.8	12.8	−4

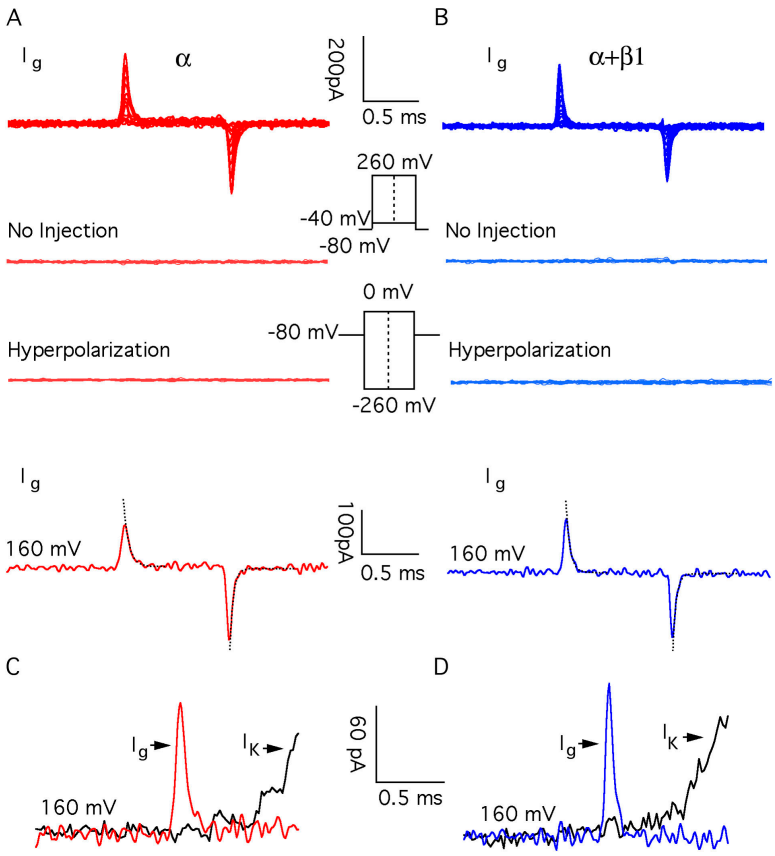

Figure 3. BK_{Ca} gating currents. (Top traces) Gating current families recorded from BK_{α} (A) and $BK_{\alpha+\beta1}$ (B) channels with 0.5 nM internal Ca^{2+}. The second and third traces in A and B demonstrate that gating currents are not observed in patches from oocytes that were not injected with BK_{Ca} cRNA (second) or with hyperpolarizing voltage steps (third). The lowest traces in A and B are gating currents recorded with pulses to +160 mV. Repolarizations are to −80 mV. Exponential fits to the on and off currents are indicated with dashed line. (C and D) Comparisons of on-gating current (I_g) and potassium current (I_K) from BK_{α} (C) and $BK_{\alpha+\beta1}$ (D) channels. Pulses were to +160 mV. Ca^{2+} = 0.5 nM. The gating and ionic currents compared in C and D are from different patches.

deed gating currents, as they are not seen in uninjected oocytes (second trace down). They are not seen in response to voltage pulses of equal magnitude but opposite polarity (third trace down), and they have characteristics very similar to those reported previously for the BK_{α} channel (Horrigan and Aldrich, 1999, 2002) (Table II).

As shown in Fig. 3 B, we also recorded gating currents from channels composed of both α and β1 subunits, and remarkably they look very much like the BK_{α} currents. They are small and fast (see fourth traces down in Fig. 3, A and B; $\tau(on) = 54.7 \pm 2.6$ μs, $n = 13$, at +160 mV; $\tau(off) = 34.6 \pm 3.0$ μs, $n = 14$, at −80 mV), which is interesting because β1 slows ionic current relaxations (see Fig. 1, A and B and Fig. 7). Clearly, however, this slowing does not arise from a slowing of voltage sensor movement.

The gating currents we have recorded from both BK_{α} and $BK_{\alpha+\beta1}$ channels have relaxation time constants close to the theoretical time resolution of our recording system $\tau \sim 40$ μs, and so we have not analyzed the kinetics of these currents further, as they may be distorted by our hardware. What is clear, however, is that both with and without β1, BK_{Ca} gating currents are very fast.

An important consequence of the speed of the BK_{α} and $BK_{\alpha+\beta1}$ channels' gating charge movement is illustrated in Fig. 3 (C and D). In response to a strong depolarization, both channels' voltage sensors move almost completely (I_g) before the channels begin to open (I_K). The time constants of channel opening are 18 (BK_{α}) and 177 ($BK_{\alpha+\beta1}$) times larger than those of gating charge movement. Thus, for both channels, rapid ON gating currents reflect voltage sensor movement in the channel's closed conformation (Stefani et al., 1997; Horrigan and Aldrich, 1999).

To determine Q–V relations we integrated both ON and OFF gating currents and plotted these integrals separately as a function of test potential. These integrals report the amount of gating charge that moves rapidly during each voltage pulse. Examples of Q–V curves from individual BK_{α} and $BK_{\alpha+\beta1}$ patches are shown in Fig. 4 (A and B), and as is evident, both with and without β1, there is very little difference between the BK_{Ca} channels' rapid ON and OFF Q–V curves. Thus, charge is not immobilized by depolarization in either case.

ON Q–V relations for each channel type were fitted with Boltzmann functions (Table III), and these curves were normalized to their maxima and averaged to yield the curves shown in Fig. 4 C. Of central importance, the two curves have the same shape, but the $BK_{\alpha+\beta1}$ curve lies far to the left of the BK_{α} curve. Indeed, both curves are well fitted by Boltzmann functions, which

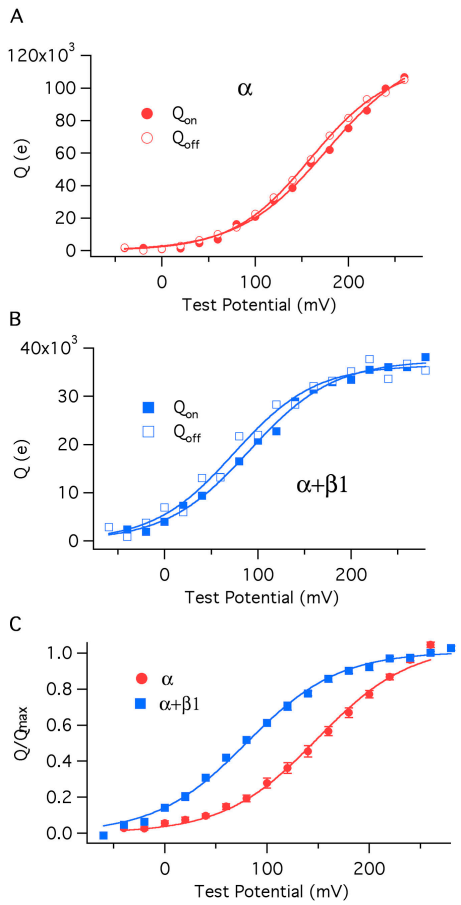

Figure 4. The β1 subunit shifts the closed channel's charge–voltage (Q–V) relation leftward without changing its shape. (A) On and Off Q–V relations determined from a single BK_{α} channel patch. (B) On and Off Q–V relations determined from a single $BK_{\alpha+\beta1}$ channel patch. (C) Normalized averaged Q_{on}–V relations for the BK_{α} (11 curves averaged) and $BK_{\alpha+\beta1}$ channels (14 curves averaged). Each curve in C is fitted with a Boltzmann function. The fit parameters are as follows: BK_{α}: $z_J = 0.577 \pm 0.023$e, $V_{hc} = 151 \pm 1.9$ mV; $BK_{\alpha+\beta1}$: $z_J = 0.571 \pm 0.025$ *e*, $V_{hc} = 80 \pm 2.4$ mV. The error bars in C represent SEM.

suggests that each channel's voltage sensors move independently, and a single voltage sensor behaves like a two-state system (Horrigan and Aldrich, 1999). For the BK_{α} channel, the fit yielded values of $V_{1/2} = 151$ mV and $z = 0.577$ *e* (for standard deviations of fit parameters see figure legends). These values are very similar to those published previously for BK_{α} gating currents (Horrigan and Aldrich, 1999, 2002) (Table II). The $BK_{\alpha+\beta1}$ fit yielded values of $V_{1/2} = 80$ mV and $z = 0.571$ *e*. Thus, β1 does not change the voltage sensor's gating charge, as has been suggested (Cox and Aldrich, 2000; Orio and Latorre, 2005), but it does shift the closed channel's Q–V relation 71 mV leftward along the voltage axis such that at physiological voltages, the $BK_{\alpha+\beta1}$ channel's voltage sensors are much more often in their active configuration.

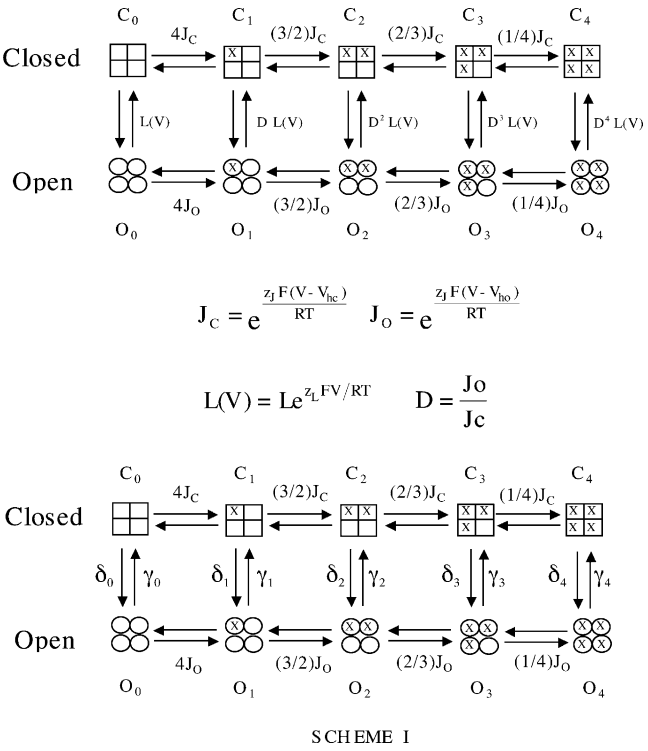

Figure 5. The allosteric model of BK_{Ca} voltage-dependent gating of Horrigan et al. (1999). Horizontal transitions represent voltage senor movement. Vertical transitions represent channel opening. For details of the model see RESULTS and MATERIALS AND METHODS.

The Current View of BK_{α} Voltage-dependent Gating

It is useful to view these results in the context of the current view of BK_{α} voltage-dependent gating. A model represented by Scheme I (Fig. 5) has been shown by Horrigan, Cui, and Aldrich to very well approximate BK_{α} gating and ionic currents in the absence of Ca^{2+}, over a very wide range of voltages (Horrigan and Aldrich, 1999, 2002; Horrigan et al., 1999). Horizontal transitions represent movement of the channel's four voltage sensors, each of which can be either active or inactive. Vertical transitions represent the conformational change by which the channel opens. The activation of a voltage sensor is not required for channel opening, but rather it promotes opening by lowering the free energy difference between open and closed.

TABLE III

Comparing Q–V Parameters

	$V_{1/2}$	z	Q_{max}	n
	mV	*e*	*e*	
BK_{α}	156 ± 3.8	0.57 ± 0.02	49305 ± 6623	22
$BK_{\alpha+\beta1}$	80 ± 3.1[a]	0.57 ± 0.01	27548 ± 4327[a]	14

The values shown are Boltzmann-fit parameters. They indicate mean ± SEM. Q_{max} represents the maximum gating charge measured per patch.
[a]Statistical significance between BK_{α} and $BK_{\alpha+\beta1}$ values $P < 0.05$.

Indeed, the factor by which the movement of a voltage sensor increases the closed-to-open equilibrium constant, referred to by Horrigan, Cui, and Aldrich as D, is given simply by J_O/J_C, where J_O is the equilibrium constant for voltage sensor activation at 0 mV when the channel is open, and J_C is this equilibrium constant when the channel is closed. J_C and J_O can be related to the midpoints of the open and closed channel's Q–V relation as follows:

$$J_C = e^{\frac{z_J F(V - V_{hc})}{RT}} \quad (7)$$

$$J_O = e^{\frac{z_J F(V - V_{ho})}{RT}}, \quad (8)$$

where R, T, and F have their usual meanings, z_J is the gating charge associated with a single voltage sensor, and V_{hc} and V_{ho} are the half-maximal activation voltages of the channel's Q–V relation, when the channel is either closed (V_{hc}) or open (V_{ho}). In order for voltage sensor movement to promote opening, V_{ho} must be more negative than V_{hc}.

Completing then the mathematical description, the open probability (P_{open}) of the Horrigan, Cui, and Aldrich model as a function of voltage (V) is given by Eq. 9:

$$P_{open} = \frac{1}{1 + \frac{1}{L}\left(\frac{1 + e^{z_J F(V - V_{hc})/RT}}{1 + e^{z_J F(V - V_{ho})/RT}}\right)^4 e^{-z_L FV/RT}}, \quad (9)$$

where L is the equilibrium constant between open and closed at 0 mV when no voltage sensors are active, and z_L is a small amount of gating charge associated with the closed-to-open conformational change.

As is the case for other voltage-gated K^+ channels, it is fairly clear that the S4 region, and probably part of S3, forms the BK_{Ca} channel's voltage sensor, whose gating charge is designated here z_J (Stefani et al., 1997; Diaz et al., 1998; Horrigan and Aldrich, 1999; Hu et al., 2003). The physical basis for z_L, however, has yet to be determined, but without assigning some voltage dependence to the closed-to-open conformational change, it is not possible to fit the BK_α ionic current data at all well (Horrigan and Aldrich, 1999, 2002; Horrigan et al., 1999; Cox and Aldrich, 2000; Cui and Aldrich, 2000; Rothberg and Magleby, 2000). Thus, the equilibrium voltage dependence of BK_α gating in the absence of Ca^{2+} is well described by five parameters, V_{hc}, V_{ho}, z_J, L, and z_L, and to this point our data allows us to specify two of them V_{hc} and z_J. To fully determine the effects of β1 on the voltage-dependent aspects of BK_{Ca} channel gating at equilibrium, however, requires that we specify V_{ho}, L, and z_L for both channels as well. To do this we have performed the experiments described below.

Estimating β1's Effects on the Closed-to-Open Conformational Change

At far negative voltages, where no voltage sensors are active, Eq. 9 reduces to Eq. 10 (Horrigan et al., 1999)

$$P_{open} = Le^{z_L FV/RT}, \quad (10)$$

which can be rewritten as

$$\log(P_{open}) = \frac{0.4342 z_L FV}{RT} + \log(L). \quad (11)$$

Eq. 11 states that as we make the membrane voltage more and more hyperpolarized, a plot of $\log(P_{open})$ vs. voltage will begin to turn away from the voltage axis, and it will reach a limiting slope that is less than the maximum slope and reflects the voltage dependence of just the closed-to-open conformational change (Horrigan and Aldrich, 1999, 2002; Horrigan et al., 1999). That is, in this voltage range, the slope of the $\log(P_{open})$–V relation will be determined only by z_L, and the position of the curve on the vertical axis will be determined only by L. Thus, as has been discussed previously (Horrigan and Aldrich, 1999, 2002), by determining the BK_{Ca} channel's P_{open} vs. voltage relation at far negative potentials we can estimate z_L and L directly.

To do this, we recorded BK_α and $BK_{\alpha+\beta1}$ macroscopic currents at depolarized voltages (+10 to +80 mV) and 10 or 100 μM Ca^{2+}. From these currents we could determine the number of channels in a given patch (N) (see MATERIALS AND METHODS). Then, we lowered the Ca^{2+} concentration to 3 nM and the membrane voltage to negative values where the channels are rarely open, and recorded unitary currents. Such currents are shown in Fig. 6 (A and B). Notice, the BK_α channels appear to open more frequently than the $BK_{\alpha+\beta1}$ channels, but the burst times of the $BK_{\alpha+\beta1}$ channels appear on average longer (expanded traces). From data like that in A and B, the probabilities of observing 1, 2, 3 .... open channels at a given time were determined with all-points histograms, and these probabilities and N were then used to determine the true mean open probability of the channels in each patch (see MATERIALS AND METHODS). In this way, we could measure open probabilities as low as 10^{-6}.

$\log(P_{open})$ vs. voltage plots are shown in Fig. 6 (C and D) for the BK_α and $BK_{\alpha+\beta1}$ channels. As the voltage becomes more negative, the BK_α plot curves upward starting at ∼−60 mV, and it reaches a limiting slope by ∼−100 mV. Fitting just the most negative part of this curve with Eq. 11 yields values for L and z_L of 2.2×10^{-6} and $0.410e$ respectively, again similar to published values (Horrigan and Aldrich, 1999, 2002) (Table II) (for standard errors of fit parameters see figure legends). Surprisingly, however, in the $BK_{\alpha+\beta1}$ plot, no

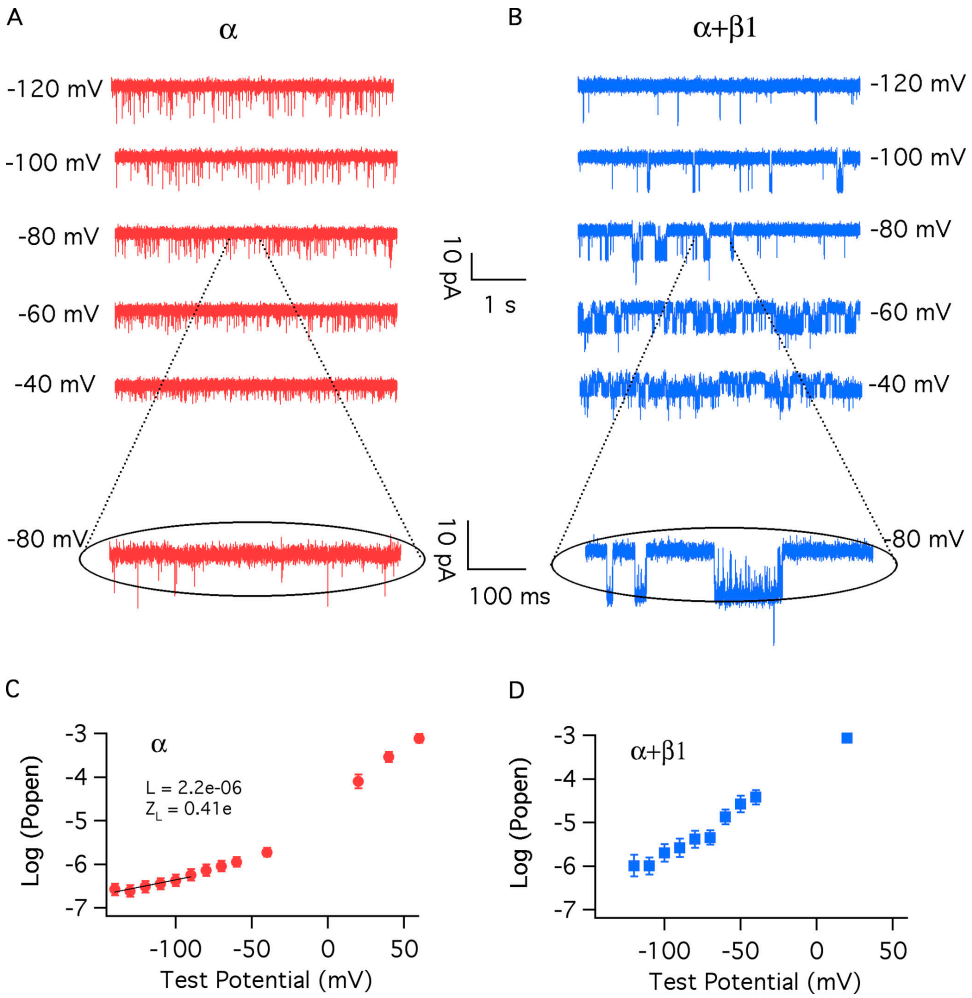

Figure 6. Estimating L and z_L from P_{open} at negative voltages. Unitary currents were recorded with 3 nM internal Ca^{2+} from BK_{α} (A) and $BK_{\alpha+\beta1}$(B) channels. The patch in A contained 2,859 channels. The patch in B contained 3,270 channels. Mean $\log(P_{open})$–voltage relations determined from patches like that in A (12 patches) and B (15 patches) are shown in C for the BK_{α} channel and D for the $BK_{\alpha+\beta1}$ channel. In C, the bottom of the curve is fitted with the following function: $\log(P_{open}) = \log(L) + 0.4342 z_L FV/RT$. The resulting parameters were $\log(L) = -5.66 \pm 0.13$, $z_L = 0.410 \pm 0.065$. In D, no submaximal limiting slope was identified.

such submaximal limiting slope is attained. Instead, down to −120 mV, the $BK_{\alpha+\beta1}$ channel's $\log(P_{open})$–V relation remains roughly linear, with no clear inflection point that would suggest that the limiting slope is being approached. This is surprising, because Scheme I suggests that such an inflection point should exist, and the fact that we do not see it argues either that the β1 subunit fundamentally alters the gating behavior of the BK_{Ca} channel such that models of the form of Scheme I no longer apply, or we have yet to examine voltages negative enough to see the inflection point. Indeed, this latter possibility seems very real, as we have already discovered that it takes significantly lower voltages to hold the channel's voltage sensors in their inactive state, at least for the closed channel, when the β1 subunit is present (Fig. 4 C). Unfortunately, however, we found it technically unfeasible to make accurate P_{open} measurements for the $BK_{\alpha+\beta1}$ channel at voltages more negative than −120 mV, where P_{open} approaches 10^{-7}. As described below, however, we have used ionic current kinetics to estimate where, if it exists, the inflection point should be.

τ-Relaxation vs. Voltage Relations Suggest No Change in z_L

But for a brief delay, the onset and offset of BK_{α} ionic currents can be well fitted with a simple exponential function over a very wide voltage range. β1 does not change this; however, at 0 Ca^{2+} it does slow both activation and deactivation. On a plot of log(τ-relaxation) vs. voltage this is seen as an upward shift in the channel's log(τ)–V curve (Fig. 7 C). The general shapes of the BK_{α} and the $BK_{\alpha+\beta1}$ curves, however, remain similar. At far negative voltages there is a shallow region of positive slope. This transitions into a steeper region that persists until the plots reach a peak, and after the peak, τ-relaxation falls often steadily at high voltages. According to the Horrigan, Cui, and Aldrich model (Fig. 5, bottom), the phases of these plots are understood as follows. At far negative voltages, no voltage sensors are active, and τ-relaxation is determined by the rate constant of the O_0 to C_0 transition and its voltage dependence (z_γ). At far positive voltages a similar situation obtains, and τ-relaxation is determined by the C_4 to O_4 rate constant and its voltage dependence (z_δ); where $z_\delta + z_\gamma = z_L$. In the middle, no single transition determines the time

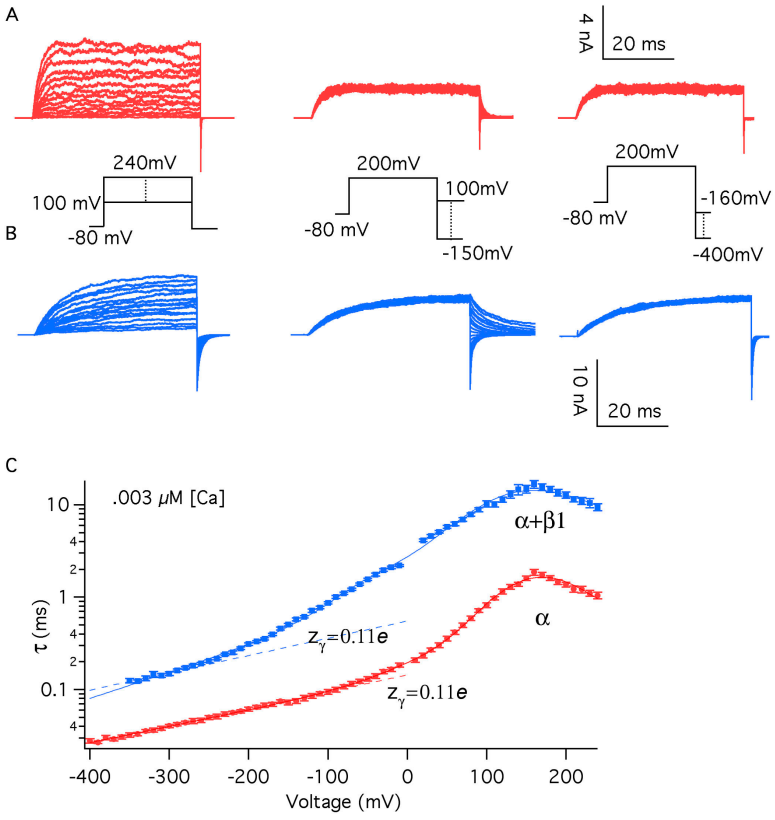

Figure 7. The β1 subunit does not alter the voltage dependence of the closed-to-open conformational change. Macroscopic ionic currents were recorded from BK_α (A) and $BK_{\alpha+\beta1}$ (B) channels in excised oocyte macropatches. Voltage steps were varied as indicated, and the time courses of relaxation were fitted with single-exponential functions. Time constants (τ) from the fits are plotted in C. For voltages of +100 mV and greater, activation time constants are plotted. Otherwise deactivation time courses are plotted. The τ–V curves in C were fitted (solid lines) to a function that approximates the kinetics of Scheme I in the limit that voltage sensor movement is fast relative to channel opening and closing (see MATERIALS AND METHODS). The fit parameters were as follows: BK_α: held V_{hc}=151 mV, L = 2.2 × 10^{-6}, z_J = 0.58 *e*, z_L = 0.41 *e*, fitting yielded D = 12.6 ± 0.43, z_γ = 0.10 ± 0.002 *e*, $\gamma0(0)$ = 7452.3 s^{-1}, $\gamma1(0)$ = 4121.4 s^{-1}, $\gamma2(0)$ = 5645.8 s^{-1}, $\gamma3(0)$ = 851 s^{-1}, $\gamma4(0)$ = 1025 s^{-1}, $\delta0(0)$ = 0.016 s^{-1}, $\delta1(0)$ = 0.114 s^{-1}, $\delta2(0)$ = 1.98 s^{-1}, $\delta3(0)$ = 3.76 s^{-1}, $\delta4(0)$ = 57.12 s^{-1}; $BK_{\alpha+\beta1}$: held V_{hc} = 80 mV, z_J = 0.57 *e*, fitting yielded L = 3.3 × 10^{-6} ± 6.4 × 10^{-6}, z_L = 0.46 *e*, D = 10.4 ± 6.4, z_γ = 0.17 *e*, $\gamma0(0)$ = 931.7 s^{-1}, $\gamma1(0)$ = 213.2 s^{-1}, $\gamma2(0)$ = 547.8 s^{-1}, $\gamma3(0)$ = 333.5 s^{-1}, $\gamma4(0)$ = 126.7 s^{-1}; $\delta0(0)$ = 0.003 s^{-1}, $\delta1(0)$ = 0.007 s^{-1}, $\delta2(0)$ = 0.198 s^{-1}, $\delta3(0)$ = 1.251 s^{-1}, $\delta4(0)$ = 4.934 s^{-1}. Both curves are also fitted (dashed lines) at far negative voltages with the following function:

$$\tau = \frac{1}{\gamma(0)e^{-z_\gamma FV/RT}}.$$

Fit parameters are as follows: BK_α (voltages <−180 mV) $\gamma(0)$ = 6940.8 s^{-1}, z = 0.11 *e*; $BK_{\alpha+\beta1}$ (voltages <−280 mV) $\gamma(0)$ = 1808.7 s^{-1}, z_γ = 0.11 *e*.

constant of relaxation; but rather, as voltage sensors become active, a weighted average of all the vertical rate constants in Scheme I prevails. Thus, just as with the log(P_{open})–V relation, the model predicts that there will be a transition or inflection point in the channel's log(τ)–V relation at the voltage where voltage sensors start to become activated, and at voltages more negative than this the plot will reach a limiting slope that reflects now the portion of z_L associated with the closing transition (z_γ) (Horrigan and Aldrich, 2002).

Viewing Fig. 7 C in this light, then, the BK_α curve has a limiting positive slope of ∼0.11*e* (dashed line), which suggests that z_γ = 0.11 *e*, and it starts to veer upward at ∼−60 mV, which, as expected, is the same position as the inflection point in the BK_α channel's log(P_{open})–V curve (Fig. 6 C). Interestingly, however, the $BK_{\alpha+\beta1}$ curve appears to reach the same limiting slope at negative voltages as does the BK_α curve (dashed lines), so z_γ appears unchanged by β1. And, at the most positive voltages tested (although here it is not clear that limiting voltages have been reached) the two curves also have the same slope, which suggests that z_δ is also little altered. Thus, β1 does not appear to affect z_L, and we can estimate that it is ∼0.41*e* for both channels. Indeed, apart from their position on the ordinate, the essential difference between the two curves in Fig. 7 C is the position of their inflection point; the $BK_{\alpha+\beta1}$ channel's lies ∼140 mV farther negative. In fact, the $BK_{\alpha+\beta1}$ inflection point it is at ∼−200 mV, which is out of the voltage range of our P_{open} measurements in Fig. 6 D. Thus, there is an inflection point when the channel contains β1, and its large negative value further supports the notion that β1 shifts voltage sensor activation to more negative voltages. Furthermore, as the time constant of relaxation at negative voltages is determined primarily by the distribution of active voltage sensors in the open channel (Cox et al., 1997a; Horrigan and Aldrich, 2002), this result suggests that β1 shifts the channel's Q–V relation leftward on the voltage axis when the channel is open.

Estimating L and V_{ho} With and Without β1

To this point then we have specified V_{hc}, z_J, and z_L for both channels, and left to specify are V_{ho} for the BK_α channel, and V_{ho} and *L* for the $BK_{\alpha+\beta1}$ channel. One way we have attempted to estimate these parameters is to fit the two curves in Fig. 7 C with Eq. 12 below, which approximates Scheme I's τ–V relation in the limit that volt-

age sensor movement is much faster than channel opening and closing (Cox et al., 1997a; Horrigan and Aldrich, 2002; for details of the approximation see MATERIALS AND METHODS). As this condition applies for both channels over much of the voltage range, such an approximation is likely to be reasonably good. Indeed, Eq. 12 fits both curves quite well (Fig. 7 C, solid lines).

$$\tau(I_K) = \left(\sum_{i=0}^{4}\gamma_i f_{Oi} + \sum_{i=0}^{4}\delta_i f_{Ci}\right)^{-1} \qquad (12)$$

Here δ_i and γ_i are the forward and backward rate constants enumerated in Fig. 7 (bottom) and f_{Oi} and f_{Ci} represent the fraction of open channels or closed that occupy state O_i or C_i respectively. In fitting the BK_α log(τ)–V curve we held V_{hc}, z_J, L, and z_L to the values we estimated from gating current and limiting P_{open} measurements, leaving only V_{ho} to vary along with z_γ and five rate constants, one for each vertical step in Scheme I. The resulting fit yielded $z_\gamma = 0.11$ and $V_{ho} = +39$ mV. For the $BK_{\alpha+\beta1}$ fit we adjusted V_{hc} to the value we obtained from our $BK_{\alpha+\beta1}$ gating current measurements, +80 mV, z_J was again fixed, and L was now allowed to vary freely along with z_L, V_{ho}, z_γ, and again five rate constants. The resulting fit yielded $V_{ho} = -25$ mV, $z_\gamma = 0.15$, and $L = 3.3 \times 10^{-6}$, $z_L = 0.46$ (for standard deviations of fit parameters see figure legend). Thus, this analysis suggests, as we surmised above, that z_L and z_γ change little, if any, with β1 coexpression, but that V_{ho} moves ~64 mV leftward, while L perhaps increases slightly ($2.2 \times 10^{-6} \rightarrow 3.3 \times 10^{-6}$) but remains on the order of 10^{-6}.

A more direct way to measure V_{ho} for either channel would be to measure gating charge movement exclusively when the channel is open. This, however, requires large prolonged depolarizations that we have found technically unfeasible. Another way we can estimate V_{ho}, however, and indeed also L for the $BK_{\alpha+\beta1}$ channel, is to simply fit each channel's P_{open}–V relation with Eq. 9, while holding the parameters we have already determined constant. Since for the BK_α channel we have specified four of five parameters, and for the $BK_{\alpha+\beta1}$ channel three of five, we expect such fits to be very well constrained.

To do this we combined our limiting P_{open} data (Fig. 6) with macroscopic current data (Fig. 2 G) to obtain P_{open}–V curves that are well determined over large ranges of both voltage and P_{open}. Fig. 8 shows these curves fitted with Eq. 9. For the BK_α fit in A, V_{hc}, z_J, L, and z_L were set to the following values: $z_J = 0.58$ e, $V_{hc} = 151$ mV, $z_L = 0.41$ e, $L = 2.2 \times 10^{-6}$, and D was allowed to vary freely. This yielded $D = 16.8$, which indicates a V_{ho} value of +27 mV, similar to a previous report (Horrigan and Aldrich, 1999) (Table II). Similarly, for the $BK_{\alpha+\beta1}$ fit (Fig. 8 B, solid line), V_{hc}, z_J, and z_L were set as follows: $z_J = 0.57$ e, $V_{hc} = 80$ mV, $z_L = 0.41$ e, and the fit

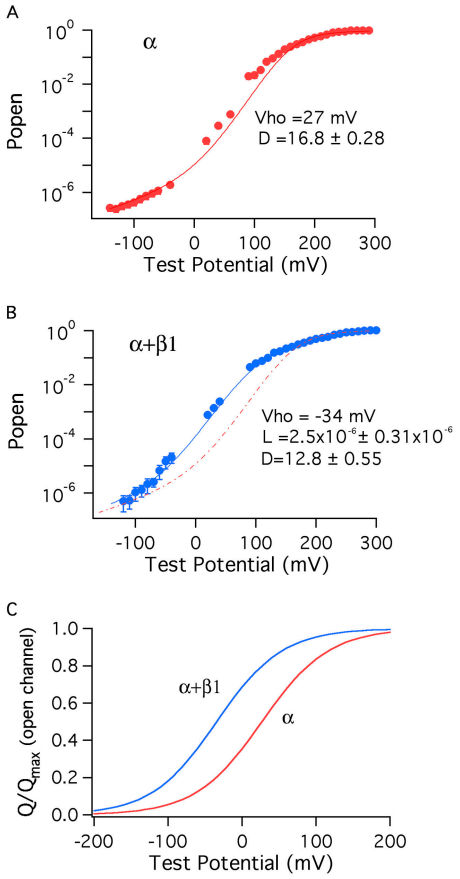

Figure 8. Estimating L and V_{ho} from P_{open}–V curve fits. (A) The P_o–V relation of the BK_α channel at 3 nM Ca^{2+} is shown over a wide range of voltages. At +60 mV and below, the data points are from unitary current measurements; above +60 mV, the data are from macroscopic current measurements. The curve displayed represents the average of 35 experiments, and error bars represent SEM. The data are fitted with Eq. 9 as described in RESULTS. Free parameters: D = 16.8 ± 0.28. (B) The P_o–V relation of the $BK_{\alpha+\beta1}$ channel. The curve displayed represents the average of 43 experiments, and error bars represent SEM. As in A, the data are fitted with Eq. 9. Free parameters: D = 12.8 ± 0.55, L = $2.53 \times 10^{-6} \pm 0.55 \times 10^{-6}$. The dashed red curve is the fit from A placed here for ease of comparison. (C) Simulated Q–V relations for the open BK_α and $BK_{\alpha+\beta1}$ channels demonstrating the −61 mV shift induced by β1 that the fits in A and B predict. The functions displayed are

$$\frac{Q}{Q_{max}} = \frac{1}{1 + e^{z_J F(V_{ho} - V)/RT}},$$

with V_{ho} equal to 27 mV (BK_α) and −34 mV ($BK_{\alpha+\beta1}$) and $z_J = 0.58$ (BK_α), $z_J = 0.57$ ($BK_{\alpha+\beta1}$).

yielded a D value of 12.8 that equates to $V_{ho} = -34$ mV, and $L = 2.5 \times 10^{-6}$. Thus β1 is estimated here to shift V_{ho} leftward 61 mV (see simulations in Fig. 8 C) but it has almost no effect on L.

To this point then our conclusions are strikingly simple. The β1 subunit has little or no effect on the equilibrium constant of the conformational change by which the BK_{Ca} channel opens, and it does not affect

the gating charge on the channel's voltage sensors, but it does stabilize voltage sensor activation both when the channel is open and when it is closed such that voltage sensors activate at more negative voltages with β1 present. Furthermore, β1 more effectively stabilizes the active voltage sensor when the channel is closed, than when it is open. That is, $||\Delta V_{hc}|| > ||\Delta V_{ho}||$, and this reduces D the factor by which voltage sensor activation promotes channel opening by 24%, from 16.8 to 12.8.

β1 Affects Ca^{2+} Binding

The question still remains, however, as to whether these changes are enough to explain the changes in Ca^{2+} sensitivity described in Figs. 1 and 2. To address this issue we have incorporated our findings into a model of BK_{Ca} channel gating that takes into account both Ca^{2+} and voltage sensing.

Our recent work suggests that the BK_{Ca} channel has two sets of four high-affinity Ca^{2+} binding sites, which are structurally distinct but have similar binding properties (Bao et al., 2002, 2004; Xia et al., 2002). Assuming one site does not affect another, and the channel's voltage sensors and Ca^{2+} binding sites also act independently, this information can be combined with Scheme I to produce a model of BK_{Ca} channel gating that considers both Ca^{2+} binding and voltage sensing (Cox and Aldrich, 2000; Cui and Aldrich, 2000; Rothberg and Magleby, 2000; Zhang et al., 2001; Horrigan and Aldrich, 2002). The open probability of such a model is given by Eq. 13:

$$P_{open} = \frac{1}{1+\left(\frac{1+e^{z_J F(V-V_{hc})/RT}}{1+e^{z_J F(V-V_{ho})/RT}}\right)^4\left(\frac{1+([Ca]/K_{C1})}{1+([Ca]/K_{O1})}\right)^4\left(\frac{1+([Ca]/K_{C2})}{1+([Ca]/K_{O2})}\right)^4\left(\frac{1}{L}\right)e^{-z_L FV/RT}}, \quad (13)$$

where now, as compared with Eq. 9, two terms has been added to the denominator that each contain a set of Ca^{2+} dissociation constants, one set for each binding site (K_{C1}, K_{O1}; K_{C2}, K_{O2}). Here, Ca^{2+} binding promotes opening by binding more tightly to the open channel than the closed, and thus two constants are specified for each type of site. The *c* subscript denotes the closed channel and the *o* subscript, the open channel. Because, both types of binding sites appear to have similar binding properties, we may simplify Eq. 13 to Eq. 14:

$$P_{open} = \frac{1}{1+\left(\frac{1+e^{z_J F(V-V_{hc})/RT}}{1+e^{z_J F(V-V_{ho})/RT}}\right)^4\left(\frac{1+[Ca]/K_C}{1+[Ca]/K_O}\right)^8\left(\frac{1}{L}\right)e^{-z_L FV/RT}}, \quad (14)$$

where now eight equivalent binding sites are considered with binding constants K_C and K_O.

To see, then, if the changes in V_{hc} and V_{ho} that we have observed upon β1 coexpression are sufficient to account for the BK_α channel's enhanced Ca^{2+} response, for each channel type, we fitted a series of G–V relations with Eq. 14 (Fig. 9). For the BK_α fit (Fig. 9 A), V_{hc}, V_{ho}, z_J, L, and z_L were held at the values we determined from our experiments in the absence of Ca^{2+} (Table II), and only K_C and K_O were allowed to vary. Still a reasonably good fit was obtained that captured well the shifting nature of the BK_α channel's G–V relation as a function of Ca^{2+} concentration. This fit yielded $K_C = 3.71$ μM and $K_O = 0.88$ μM, similar to our previous estimates (Bao et al., 2002).

When the BK_α fit is placed on the $BK_{\alpha+\beta1}$ data, of course it does not fit at all well (Fig. 9 B). Next, however, we adjusted V_{hc} and V_{ho} and L to mimic the effects of β1. V_{hc} was moved from +151 to +80 mV, V_{ho} was moved from +27 to −34 mV, and L was increased slightly, from 2.2×10^{-6} to 2.5×10^{-6}. The important result is shown in Fig. 9 C. The effects of β1 on voltage sensing do greatly improve the G–V fits at low Ca^{2+} concentrations, 1 and 0.003 μM. But at higher concentrations, the fit is not good, and it gets progressively worse as the Ca^{2+} concentration is increased. High Ca^{2+} concentrations do not shift the model's G–V relation far enough leftward. Thus, β1's effects on voltage sensing appear important, but they are not sufficient to account for all of the $BK_{\alpha+\beta1}$ channel's enhanced Ca^{2+}sensitivity.

To determine then what is required to fully account for the $BK_{\alpha+\beta1}$ G–V relation as a function of Ca^{2+}, we fit the $BK_{\alpha+\beta1}$ G-V relations with Eq. 14, now fixing the voltage-sensing parameters to their $BK_{\alpha+\beta1}$ values ($V_{hc} = 80$ mV and $V_{ho} = -34$ mV, L = 2.5×10^{-6}, $z_L = 0.41$) and allowing K_C and K_O to vary. The resulting fit is shown in Fig. 9 D. To account for the additional leftward shifting K_C increases from 3.71 to 4.72 μM, while K_O declines slightly from 0.88 to 0.82 μM. This causes the ratio K_C/K_O to increase from 4.2 to 5.7.

Thus, our analysis suggests that β1 has a very small effect (<10%) or perhaps no affect on Ca^{2+} binding when the channel is open, consistent with our earlier study (Cox and Aldrich, 2000), and it reduces the affinity of each binding site for Ca^{2+} when the channel is closed, increasing K_C ~27%. It is perhaps surprising that such small changes in affinity can have such a dramatic effect on the position of the channel's G–V relation at high Ca^{2+} concentrations, but in fact this should be expected, as at saturating Ca^{2+} the equilibrium constant between open and closed depends on the eighth power of (K_C/K_O).

Perhaps only Half of the Channel's Binding Sites Are Affected by β1

The estimates of β1's effects on K_C and K_O just offered suppose that β1 affects all binding sites equally. However, the BK_{Ca} channel is thought to have two types of

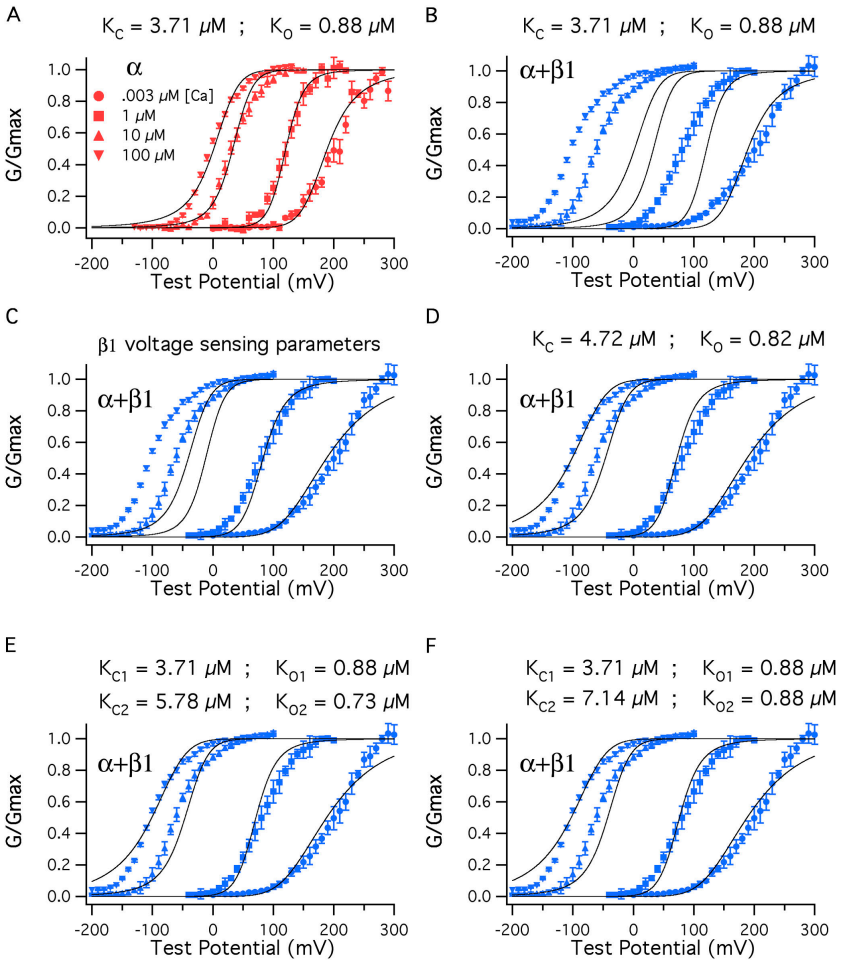

Figure 9. β1 also affects Ca^{2+} binding. (A) BK_α G–V relations at a series of Ca^{2+} concentrations fitted simultaneously (solid curves) with Eq. 14. Only K_C and K_O were allowed to vary. The fit yielded K_C = 3.71 μM and K_O = 0.88 μM. The other parameters of the fit were determined from experiments performed with nominally 0 Ca^{2+} (3 nM) (V_{hc} = 151 mV, $L = 2.2 \times 10^{-6}$, V_{ho} = 27 mV, z_J = 0.58, z_L = 0.41). (B) The fit from A is superimposed on a series of $BK_{\alpha+\beta1}$ G–V curves. (C) The voltage-sensing parameters of the model were altered to reflect the changes that occur as β1 binds, V_{ho} = (27→−34 mV), V_{hc} = (151→80 mV), L = ($2.2 \times 10^{-6} \rightarrow 2.5 \times 10^{-6}$). (D) With $BK_{\alpha+\beta1}$ voltage-sensing parameters K_C and K_O were allowed to vary freely, yielding the fit shown and K_C = 4.72 μM, K_O = 0.82 μM. (E) Here, the $BK_{\alpha+\beta1}$ voltage-sensing parameters were used for the fit, and β1 was allowed to influence only half of the channels' eight Ca^{2+}-binding sites. The data are fit with Eq. 13. K_{C1} and K_{O1} were held at 3.71 μM and 0.88 μM, respectively. K_{C2} and K_{O2} were allowed to vary freely, yielding K_{C2} = 5.78 μM, K_{O2} = 0.73 μM. (F) The data are again fit with Eq. 13 but now K_{O2} was held at 0.88 μM and only K_{C2} was allowed to vary. This yielded K_{C2} = 7.14 μM.

high-affinity binding sites (Schreiber and Salkoff, 1997; Bao et al., 2002; Xia et al., 2002), and it could reasonably be that β1 affects only one type of site. In this case, to account for the effects of β1, the ratio K_C/K_O for the site that is affected would have to increase more. To determine how much more we fitted the $BK_{\alpha+\beta1}$ G–V data with Eq. 13, which supposes two types of Ca^{2+} binding sites, referred to as 1 and 2 (Fig. 9 E). For the fit we again used the $BK_{\alpha+\beta1}$ voltage-sensing parameters, but now we set one set of Ca^{2+}-binding constants to the values we determined for the BK_α channel (K_{C1} = 3.71 μM and K_{O1} = 0.88 μM), and we let the second set vary. This yielded a fit similar to the one that was obtained when all sites were assumed to be affected equally (see Fig. 11 D), but now, with only half the sites affected, K_{C2} increased to 5.78 μM and K_{O2} decreased to 0.73 μM. Thus, K_C increased an additional 22%, and now a larger change in K_O was also produced (0.88 μM→0.73 μM, 17% decline). To determine, however, whether this change in K_{O2} was in fact needed, we reran the fit, now also holding K_{O2} to 0.88 μM. The result is shown in Fig. 9 F. A similar fit is obtained, now with K_{C2} increased to 7.14 μM.

Thus, whether we allow all eight or only four of the model channel's Ca^{2+}-binding sites to be modified by β1, we can account for the general effects of β1 on the position of the BK_{Ca} channel's G–V relation as a function of Ca^{2+} concentration without supposing any change in K_O, and whether K_O does in fact decrease as β1 binds, we are as yet uncertain. What is clear, however, is that in order to account for the G–V shift produced by β1 at 100 μM Ca^{2+}, the closed affinity of at least one type of high-affinity Ca^{2+}-binding site must be lowered such that K_C increases between 27% and 92%.

DISCUSSION

Here we have addressed the question of how, in a biophysical sense, the BK_{Ca} β1 subunit enhances the BK_{Ca} channel's Ca^{2+} sensitivity. Because previous work suggested that much of this phenomenon may be due to effects on aspects of gating that are separate from Ca^{2+} binding (Cox and Aldrich, 2000; Nimigean and Magleby, 2000; Qian et al., 2002), we focused first on determining to what extent β1 alters various parameters that govern Ca^{2+}-independent gating. Fortunately, the

gating of the BK_α channel in the absence of Ca^{2+} had been carefully examined, and Horrigan, Cui, and Aldrich developed a model that provides both a good mathematical description of the BK_{Ca} channel's response to changes in voltage and an intuitive understanding of the various parameters that govern this process (Horrigan and Aldrich, 1999, 2002; Horrigan et al., 1999).

The Horrigan, Cui, and Aldrich model may be summarized as follows. The BK_α channel opens and closes via a single conformational change that is weakly voltage dependent. This central conformational change is indirectly, or allosterically, affected by four voltage sensors, each of which can be either active or inactive. When a voltage sensor becomes active, it promotes opening by lowering the energy of the open conformation of the channel relative to the closed. For this to occur each voltage sensor's half-activation voltage must become more negative as the channel opens.

With this model as a guide, our task then became twofold, to determine if the Horrigan and Aldrich model still describes the gating of the BK_{Ca} channel when the β1 subunit is part of the channel, and if so, to then determine how the five parameters, V_{hc}, V_{ho}, z_J, L, and z_L that govern the model' s behavior at equilibrium change upon β1 coexpression. Calculations indicate that changes in any or all of these parameters could lead to changes in the apparent affinity of the channel for Ca^{2+} at many voltages (Cox and Aldrich, 2000). To determine, however, which were actually changing, following the lead of Horrigan and Aldrich (1999), we used both gating and ionic currents to constrain the parameters of the model so that each could be well determined. Our results may be summarized as follows.

With β1 coexpression, the Horrigan, Cui, and Aldrich model (Fig. 5, Scheme I) is still applicable. β1 does not slow voltage sensor movement, which remains fast relative to opening and closing. It has very little or no effect on the parameters that govern the central conformational change at equilibrium (L and z_L), and it has no effect on the gating charge carried by each voltage sensor (z_J). It does, however, have an important effect on the energy required for voltage sensor activation, both when the channel is open and when it is closed. That is, β1 affects V_{hc} and V_{ho}, both of which are shifted tens of millivolts leftward on the voltage axis. Interestingly, however, β1 shifts V_{hc} ~10 mV further than it shifts V_{ho}, and this reduces by 24% the factor D by which voltage sensor movement influences opening. As will be discussed below, this reduction in D has consequences for the shape and position of the BK_{Ca} channel's G–V relation in the absence of Ca^{2+}.

We have also found, however, that, although changes in V_{hc} and V_{ho} can account for much of the effects of β1 on Ca^{2+} sensing at low Ca^{2+} concentrations (1 μM and below), at higher Ca^{2+} concentrations, some effect of β1 on Ca^{2+} binding must also be supposed. In particular, our data suggest that β1 either has no effect or a very small effect on the affinity of the channel's Ca^{2+} binding sites when the channel is open (a decrease in K_O from ~0.9 μM to no less than 0.7 μM), but it increases the Ca^{2+} dissociation constant of the closed channel by ~27% (3.7 to 4.7 μM), if all eight binding sites are affected, or by ~57–92% (3.7 to 5.8 μM or 7.1 μM), if only four sites are affected. These numbers correspond to a change in the factor C by which Ca^{2+} binding influences opening by 57–93%. Thus, paradoxically, $BK_{\alpha+\beta1}$ channels are more sensitive to Ca^{2+} throughout the physiological voltage range, because they bind Ca^{2+} worse when they are closed and because their voltage sensors activate at lower voltages.

β1's Effects in Energetic Terms

To gain an intuitive understanding of these results as they relate to the BK_{Ca} channel's G–V and Ca^{2+} dose–response curves (Fig. 2, A–G), we have found it useful to consider the influence of Ca^{2+} and voltage on channel gating in energetic terms. For this purpose, we may write for the eight–Ca^{2+} binding site four–voltage sensor model the following equation, which relates the free energy difference between open and closed (ΔG_{O-C}) to Ca^{2+} concentration $[Ca^{2+}]$ and membrane voltage.

$$\Delta G_{O-C} = \qquad (15)$$

$$-8RT\ln\left[\frac{1+[Ca]/K_O}{1+[Ca]/K_C}\right]-4RT\ln\left[\frac{1+e^{z_J F(V-V_{ho})/RT}}{1+e^{z_J F(V-V_{hc})/RT}}\right]-$$

$$z_L FV - RT\ln[L].$$

Eq. 15 has four terms. Term 1 represents the change in ΔG_{O-C} that occurs as Ca^{2+} is varied ($\Delta\Delta G_{O-C}$ Ca^{2+}), term 2 the change in ΔG_{O-C} that occurs as voltage sensors become active ($\Delta\Delta G_{O-C}$ VS), term 3 the influence of voltage on the central conformational change, and term 4 the intrinsic energy difference between open and closed when no Ca^{2+} ions are bound and no voltage sensors are active (Cui and Aldrich, 2000).

In Fig. 10 A, the sum of terms 3 and 4 is plotted as a function of voltage, and, as is evident, the direct influence of the membrane's electric field on the central conformational change contributes linearly to ΔG_{O-C}. Because β1 does not change L appreciably, or z_L, the same curve describes this influence for both channels, and only one curve has been drawn.

In Fig. 10 B term 2 is plotted using the gating parameters (V_{hc}, V_{ho}, z_J) we have determined for each channel type (BK_α and $BK_{\alpha+\beta1}$). Marked on the figure (numbered ticks) are the voltages at which there are an aver-

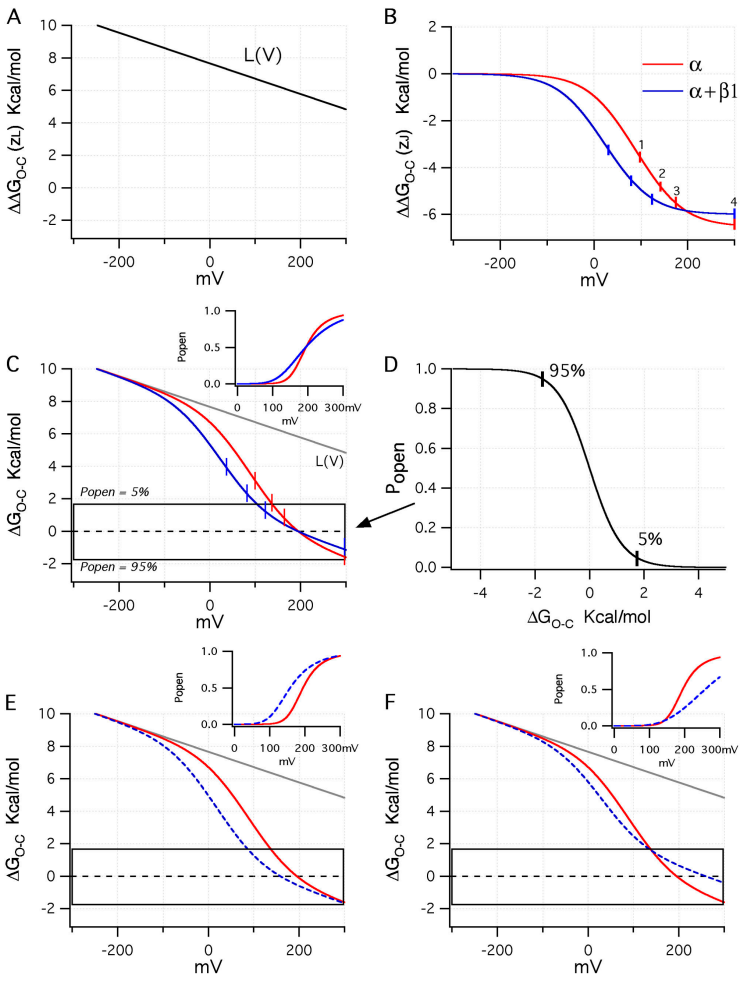

Figure 10. Examining the effects of β1 in energetic terms. (A) Plot of the sum of terms 3 and 4 from Eq. 15. (B) Plots of term 2 from Eq. 15 using either the BK_{α} (red) or $BK_{\alpha+\beta1}$ (blue) voltage-sensing parameters (Table II). (C) Plots for both channels of terms 2, 3, and 4 of Eq. 15 combined. In the inset are drawn simulated P_{open}–V curves for the BK_{α} and $BK_{\alpha+\beta1}$ channels based on the parameters in Table II and assuming 0 Ca^{2+}. The boxed region indicates the energy range over which P_{open} moves from 0.05 (top of box) to 0.95 (bottom of box). A full P_{open} vs. ΔG_{O-C} is shown in D. In E, a plot is shown like that in C except that V_{ho} for the $BK_{\alpha+\beta1}$ channel has been set to −44 mV such that V_{hc} and V_{ho} shift equally upon β1 coexpression. (F) Here V_{ho} for the $BK_{\alpha+\beta1}$ channel has been set to −20 mV to mimic a larger change in the coupling factor D upon β1 coexpression.

age of 1, 2, 3, or 4 active voltage sensors (although individual channels may have more or less). Here we see that voltage sensor movement influences opening at lower voltages, when β1 is present, but the maximum influence that voltage sensor movement can have on ΔG_{O-C}, and therefore opening, is ~7.2% less. This is due to the smaller difference between V_{hc} and V_{ho} in the $BK_{\alpha+\beta1}$ channel, which leads to a reduction in D. Indeed, in the high voltage limit, term 2 becomes simply

$$\Delta\Delta G_{O-C}(VS) = -4RT\ln\left[\frac{e^{zFV_{hc}/RT}}{e^{zFV_{ho}/RT}}\right] = -4RT\ln[D]. \quad (16)$$

Also worth noting, at the bottoms of these curves, where nearly all four voltage sensors are active, the relationship between a change in membrane voltage and a change in ΔG_{O-C} becomes quite shallow, while in the middle of these curves, it is much steeper.

Combining now terms 2, 3, and 4 yields the plot in Fig. 10 C, which describes the energetics of gating in the absence of Ca^{2+}. Superimposed on the plot is a box that indicates the range of ΔG_{O-C} over which the channel's open probability is between 5% (upper edge) and 95% (lower edge, for the complete relation; Fig. 10 D). Outside the box, changes in ΔG_{O-C} have little effect on P_{open}, while the progress of each curve through the box describes channel activation with voltage. At the dashed centerline $\Delta G_{O-C} = 0$ and thus $P_{open} = 0.5$, so the voltage at which each curve intersects this line indicates each channel's $V_{1/2}$.

β1 and the G–V at 0 Ca^{2+}?

With these plots in mind, then, we may consider such questions as why is the $BK_{\alpha+\beta1}$ G–V relation at 0 Ca^{2+} less steep than that of the BK_{α} channel? And what determines the size of the β1-induced G–V shift? And why does it increase as Ca^{2+} is raised?

Beginning with the first question, we see in Fig. 10 C that in the absence of Ca^{2+}, the $BK_{\alpha+\beta1}$ curve (blue) traverses the gating box at a shallower angle than does the BK_{α} curve (red). This makes the $BK_{\alpha+\beta1}$ channel's P_{open}–V relation shallower than that of the BK_{α} channel, and it creates a crossover between the two channels' ΔG_{O-C}–V and P_{open}–V curves (see inset). Thus, the models recapitulate the data. This type of plot, however, makes it readily apparent why. The $BK_{\alpha+\beta1}$ chan-

nel's G–V relation is shallower primarily because β1 reduces *D*, and this brings the shallow part of the $BK_{\alpha+\beta1}$ channel's $\Delta\Delta G_{O-C}$–V relation (Fig. 10 B), now combined with *L(V)* to yield its ΔG_{O-C}–V relation (Fig. 10 C), into the gating box, while in the BK_{α} channel the larger influence of voltage sensor movement on channel opening places less of this shallow region in the box. Or to put it another way, when β1 is present, the effect of voltage sensor movement on ΔG_{O-C} is reduced, and this causes the channel's P_{open}–V relation in the absence of Ca^{2+} to reflect in larger part the shallow voltage dependence of the central conformational change. Thus, in the absence of Ca^{2+}, β1 reduces the BK_{Ca} channel's P_{open}–V slope (or equivalently its G–V slope) because it shifts V_{hc} further leftward than it shifts V_{ho}. Indeed as shown in Fig. 10 E, if this were not the case, if β1 shifted both V_{hc} and V_{ho} equally such that *D* was unchanged, no crossover would occur, and the two P_{open}–V relations would have similar slopes with the $BK_{\alpha+\beta1}$ curve now standing to the left of the BK_{α} curve (see inset).

Differences between Mouse and Bovine β1 at 0 Ca^{2+}

The converse case it also of interest. Suppose β1 shifted V_{ho} less than we have found it does, say −47 mV rather than −61 mV, while still shifting V_{hc} −71 mV. In this instance (Fig. 10 F) *D* would be lowered further by β1, and the crossover point would now occur outside the gating box, such that the progress of the hypothetical $BK_{\alpha+\beta1}$ channel's ΔG_{O-C}–V curve through the box would be determined almost solely by *L(V)*. That is, in such an instance voltage sensor movement would no longer lower ΔG_{O-C} enough to be observed as a change in P_{open}, and the channel's ΔG_{O-C}–V relation and its P_{open}–V relation would reflect predominately z_L. This would cause a large rightward G–V shift upon β1 coexpression (Fig. 10 F, inset), which is interesting, because this is what we think occurs with mouse β1.

Here we have studied the effects of the bovine β1 subunit, which under most conditions are very similar to those of the mouse β1. In the absence of Ca^{2+}, however, the G–V curve of the $BK_{\alpha+\beta1mouse}$ channel is much further right shifted than that of the $BK_{\alpha+\beta1bovine}$ channel, and it has a much shallower slope (unpublished data). We suggest therefore that perhaps mouse β1 reduces *D* more than does bovine β1, and this gives rise to their different effects at 0 Ca^{2+}. Indeed, the BK_{Ca} β4 subunit also produces a large rightward G–V shift in 0 Ca^{2+}, perhaps for the same reason (Ha et al., 2004).

More generally, however, our data suggest that in the absence of Ca^{2+}, the energy imparted to BK_{Ca} channel opening by its voltage sensors (when combined with the effect of voltage on the central conformational change) is just enough to influence opening, but small changes in either the amount of energy required to open the channel (changes in *L*, or the addition of Ca^{2+}), or how much energy each voltage sensor's movement contributes to channel opening (changes in *D*), are expected to have a profound effect on the shape and position of the BK_{Ca} channel's P_{open}–V relation.

β1's Effect on the BK_{Ca} G–V curve as a Function of Ca^{2+}

Looking again at Fig. 10 C, what is also evident is that if the two ΔG_{O-C}–V curves were shifted downward, steeper parts of each curve would traverse the gating box, and the $BK_{\alpha+\beta1}$ curve would lie significantly to the left of the BK_{α} curve. Indeed, this is what occurs with Ca^{2+} binding. Term 1 of Eq. 15 is plotted in Fig. 11 A as a function of Ca^{2+}. Here we see that as the Ca^{2+} concentration increases, Ca^{2+} binding lowers ΔG_{O-C} for the BK_{α} channel ~6.7 kcal/mol, similar to what voltage sensor movement does (Fig. 10 B), while, owing to its larger K_C value, it lowers ΔG_{O-C} for the $BK_{\alpha+\beta1}$ ~8.2 kcal/mol, 22% more. On a plot of ΔG_{O-C} vs. voltage, Ca^{2+} binding is seen as a downward shift along the energy axis, with a larger shift for higher Ca^{2+}. 1 μM Ca^{2+}, for example, shifts both channel's ΔG_{O-C}–V curves downward 2.4 to 2.8 kcal/mol, such that they each now pass through the gating box at a steeper angle (Fig. 11 C). Thus, for both channels, the increase in G–V steepness observed between 0 and 1 μM Ca^{2+} (Fig. 2, C and D) is seen here to be due to Ca^{2+} lowering the energy that the voltage sensors must supply to open the channel that brings a steeper region of the $\Delta\Delta G_{O-C}$–V relation (Fig. 10 B) into the gating box. The $BK_{\alpha+\beta1}$ ΔG_{O-C}–V curve, however, now lies to the left of the BK_{α} curve, because the $BK_{\alpha+\beta1}$ channel's voltage sensors are activated at lower voltages.

Notice also in Fig. 11 C that the $BK_{\alpha+\beta1}$ curve is shifted downward by Ca^{2+} slightly more than is the BK_{α} curve, but at 1 μM Ca^{2+} this effect is not of importance, and if this were not the case (dashed line) the observed G–V shift due to β1 coexpression would be very close to the same. At higher Ca^{2+} concentrations, however, (Fig. 11, D and E), two things become evident. The downward shifting effect of Ca^{2+} on both curves means that there will be a leftward G–V shift in response to increases in Ca^{2+} for both channels, but now, as Ca^{2+} is increased, the shift will become progressively larger for the $BK_{\alpha+\beta1}$ channel. This is due to the β1-induced increase in K_C. In fact, indicated with a dashed line in Fig. 11 (D and E) is the ΔG_{O-C}–V curve that would be observed for the $BK_{\alpha+\beta1}$ channel if β1 affected only voltage sensing. Thus, at 10 μM Ca^{2+}, there would still be a leftward G–V shift in response to β1 coexpression, but it would not be nearly as far. To highlight this point further, in Fig. 11 F we have plotted the β1-induced $V_{1/2}$ shift predicted by the BK_{α} and $BK_{\alpha+\beta1}$ model channels at 0, 1, 10, and 100 μM Ca^{2+}, and indicated are the percentages of each shift that is due to β1's effects on voltage

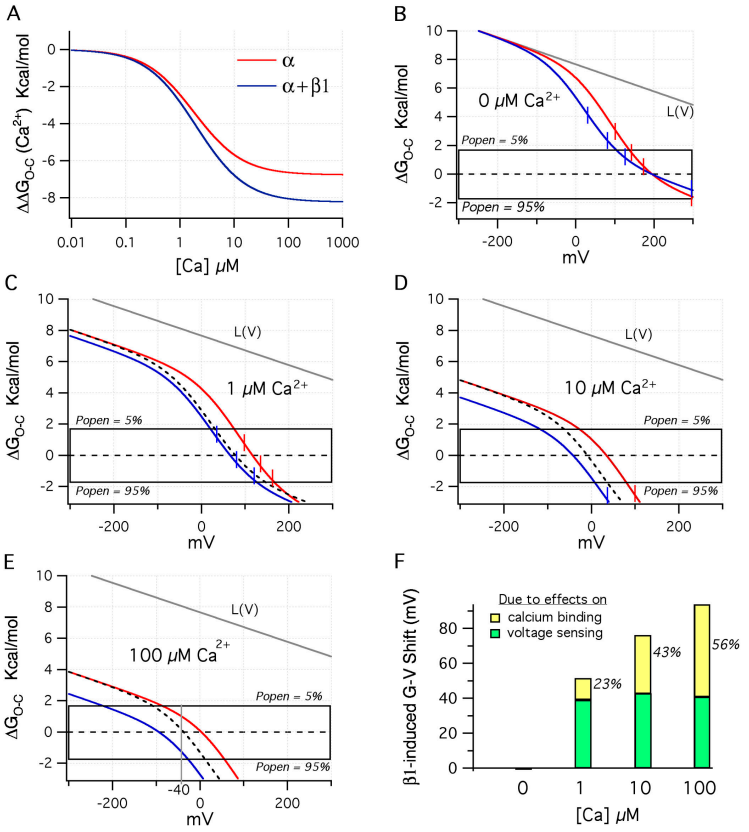

Figure 11. Ca^{2+} shifts the ΔG_{O-C}–V relations to lower energies. (A) Plot of ΔG_{O-C} vs. Ca^{2+} concentration for the BK_{α} (red) and $BK_{\alpha+\beta1}$(blue) channels using the Ca^{2+} binding parameters determined from Fig. 11 (A and D). The plots were calculated using term 1 of Eq. 15. (B) As in Fig. 10 C, plotted here are the two model channel's ΔG_{O-C}–V relations in the absence of Ca^{2+}. (C) The same relations now with 1 μM Ca^{2+}, (D) 10 μM Ca^{2+}, and (E) 100 μM Ca^{2+}. The dashed lines in C, D, and E indicate the $BK_{\alpha+\beta1}$ curve that would be observed, if there were no changes in Ca^{2+} bindng upon β1 coexpression. (F) Plotted are the total $V_{1/2}$ shifts predicted by the BK_{α} and $BK_{\alpha+\beta1}$ model channels upon β1 coexpression at 0, 1, 10, and 100 μM Ca^{2+}. In green is the percent of the total shift due to changes in voltage sensing, and in yellow is the percentage due to changes in Ca^{2+} binding.

sensing (green) and Ca^{2+} binding (yellow). Thus, according to our analysis, the leftward G–V shifts observed in Fig. 2 (D–G) are due to β1's effects on both voltage sensing and Ca^{2+} binding. At low Ca^{2+} concentrations, effects on voltage sensing are of primary importance, but at higher Ca^{2+} concentrations, the percentage of each G–V shift that is due to β1's effects on Ca^{2+} binding increases until, at 100 μM Ca^{2+}, it is just >50%.

β1's Effects on BK_{Ca} Ca^{2+} Dose–Response Curves

By picking a single voltage on these plots, we can also see why at negative voltages Ca^{2+} more effectively opens the channel when β1 is present (as shown in Fig. 2, A–C). Examining −40 mV for example, the membrane potential of typical smooth muscle myocyte, 100 μM Ca^{2+} shifts the BK_{α} ΔG_{O-C}–V curve downward such that ΔG_{O-C} (−40 mV) = 0.96 kcal/mol, which corresponds to a P_{open} of 0.164 (Fig. 11 E, gray line). With β1 present, the downward shift with 100 μM Ca^{2+} makes ΔG_{O-C} (−40 mV) = −1.34 kcal/mol, which corresponds to a P_{open} of 0.907. Thus, Ca^{2+} more effectively opens the channel at low voltages because it shifts the $BK_{\alpha+\beta1}$ channel's ΔG_{O-C}–V curve deeper into the gating box when β1 is present. Part of this is due to β1's effects on voltage sensing, in this case 41%, as if β1 only affecting voltage sensing, P_{open} at −40 mV and 100 μM Ca^{2+} would be 0.467, and part is due to its effects on Ca^{2+} binding, here 59%. At higher voltages, however, +100 mV for example, 100 μM Ca^{2+} is able to lower both ΔG_{O-C}–V curves enough to fully activate both channels, and thus no difference in maximum P_{open} is expected. But because at all voltages on average fewer bound Ca^{2+} are required to maximally activate the channel when β1 is present, at this voltage, as well as almost all others (between ∼−200 and +200 mV), the β1 subunit is expected to increase the apparent affinity of the channel for Ca^{2+}.

Our Results Relative to Previous Work

Studies by Nimigean and Magleby (1999, 2000) at the single channel level have indicated that the β1 subunit shifts the BK_{Ca} channel's Ca^{2+} dose–response curve leftward at +30 mV from an apparent affinity of 9.2 to 2.6 μM (Nimigean and Magleby, 1999 [Fig. 2 A], 2000 [Fig. 2 B]). The models of the BK_{α} and $BK_{\alpha+\beta1}$ channels we have produced predict almost an identical shift (9.3 to 2.3 μM). Furthermore, Nimigean and Magleby estimated that 80% of the shift was due to β1's effects on aspects of gating separate from Ca^{2+} binding, while 20% were due to a Ca^{2+}-dependent effect. Our models suggest a similar ratio (87% voltage sensing, 13% Ca^{2+} binding). Also they found that at +30 mV, in the absence of Ca^{2+}, β1 increases P_{open} approximately sevenfold (Nimigean and Magleby, 2000). Our models predict a 12-fold increase. Thus, on the whole, our results

are remarkably consistent with those of Nimigean and Magleby. Furthermore, they found that β1 increases P_{open} by increasing the occupancy of bursting states, which, when interpreted in terms of our results, suggests that voltage sensor activation gives rise to longer bursts of openings.

In a previous study (Cox and Aldrich, 2000) we concluded, based on macroscopic ionic current recordings, that β1 shifted V_{hc} and V_{ho} leftward, qualitatively, as we have observed, but as well probably increased L from 3.4×10^{-6} to 17.9×10^{-6} and decreased z_J from 0.51 to 0.4. Having now directly measured the movement of the channel's gating charge, however, we no longer think that z_J changes upon β1 coexpression, and if there are changes in L they are smaller than we first supposed. We also concluded in this study that β1 reduces the affinity of the channel for Ca^{2+} when it is closed, but has little or no effect on the affinity of the channel when it is open. As we have discussed, we still think this is correct.

Recently, Orio and Latorre (2005) concluded that the effects of β1 on Ca^{2+} sensing can be explained entirely by a reduction in z_J from ~0.5*e* to ~0.3*e*, with no effect on Ca^{2+} binding and no change in V_{hc}. Clearly, this idea is not consistent with our results, as with gating currents, we have directly determined the value of z_J to be 0.57*e* to 0.58*e* and unchanged by β1 coexpression, and we have found V_{hc} to be shifted 71 mV leftward by β1. Why their conclusions differ from ours is not clear, and it could be due in part to species differences between β1 subunits, as we have used bovine and they used human β1. Perhaps more important, however, in the absence of gating currents they relied in their analysis on the notion that the peak of the BK_{Ca} channel's $\tau_{relaxation}$–V relation could not remain at or near the same voltage, if V_{hc} were changing appreciably. But, as can be seen by our fits in Fig. 7 C, this statement is not correct. While it is true that changes in V_{hc} will tend to alter the position of the peak of this curve, it is also true that changes in V_{ho} can, and apparently do, counteract this effect. Also, as evidence that z_J is changing with β1 coexpression, Orio and Latorre (2005) sited a change in the maximum slope of the channel's $\ln(P_{open})$ vs. voltage relation upon β1 coexpression; however, as can be seen in Fig. 8 B (compare solid line to dashed line), we do not observe a clear change in the maximum slope of this relation upon β1 coexpression. Where our two studies agree, however, is in the finding, based in both studies on limiting-P_{open} measurements, that the voltage dependence of the central conformational changed (z_L) is unaltered by β1.

A Structural Hypothesis

While our data do not bear directly on the issue of what physical interactions between α and β1 are required for β1 to stabilize the activated voltage sensor, considerable evidence indicates that the extracellular loop common to all BK_{Ca} βs can extend over the α subunit as far as the channel's pore. The extracellular loop of β3 enters and blocks the pore in a voltage-dependent manner (Zeng et al., 2003), and the extracellular loop of β4 prevents charybdotoxin, a pore-blocking peptide, from interacting with the channel (Meera et al., 2000). Thus, it seems reasonable to suppose that the extracellular loop of β1 may interact with the external face of the α subunit as well. Indeed, perhaps it interacts with the voltage sensor at or near the top of S4. If this interaction were specific for the activated voltage sensor, than it would stabilize this position of the voltage sensor and create leftward Q–V shifts as we have observed. How much energy would it take to create such an effect? As it turns out, not very much. The 71-mV leftward V_{hc} shift we have observed with β1 coexpression corresponds to a stabilization of the active voltage sensor by only 0.9 kcal/mol, the energy of a very weak hydrogen bond or a hydrophobic interaction. Thus from an energetic point of view this idea is plausible.

Of course this hypothesis doesn't explain the effects of β1 on Ca^{2+} binding, and at this point we have none but the most general hypothesis to offer. As the physical nature of the BK_{α} channel's Ca^{2+} binding sites becomes more clear, however, perhaps how β1 influences one or more of the channel's Ca^{2+}-binding sites will become more clear as well.

This work was supported by grant R01HL64831 from the National Institutes of Health.

Olaf S. Andersen served as editor.

Submitted: 15 June 2005
Accepted: 26 August 2005

REFERENCES

Adelman, J.P., K.Z. Shen, M.P. Kavanaugh, R.A. Warren, Y.N. Wu, A. Lagrutta, C.T. Bond, and R.A. North. 1992. Calcium-activated potassium channels expressed from cloned complementary DNAs. *Neuron.* 9:209–216.

Atkinson, N.S., G.A. Robertson, and B. Ganetzky. 1991. A component of calcium-activated potassium channels encoded by the *Drosophila* slo locus. *Science.* 253:551–555.

Bao, L., A.M. Rapin, E.C. Holmstrand, and D.H. Cox. 2002. Elimination of the BK(Ca) channel's high-affinity Ca^{2+} sensitivity. *J. Gen. Physiol.* 120:173–189.

Bao, L., C. Kaldany, E.C. Holmstrand, and D.H. Cox. 2004. Mapping the BKCa channel's "Ca^{2+} bowl": side-chains essential for Ca^{2+} sensing. *J. Gen. Physiol.* 123:475–489.

Barrett, J.N., K.L. Magleby, and B.S. Pallotta. 1982. Properties of single calcium-activated potassium channels in cultured rat muscle. *J. Physiol.* 331:211–230.

Bayguinov, O., B. Hagen, J.L. Kenyon, and K.M. Sanders. 2001. Coupling strength between localized Ca^{2+} transients and K^+ channels is regulated by protein kinase C. *Am. J. Physiol. Cell Physiol.* 281:C1512–C1523.

Behrens, R., A. Nolting, F. Reimann, M. Schwarz, R. Waldschutz,

and O. Pongs. 2000. hKCNMB3 and hKCNMB4, cloning and characterization of two members of the large-conductance calcium-activated potassium channel β subunit family. *FEBS Lett.* 474:99–106.

Brenner, R., T.J. Jegla, A. Wickenden, Y. Liu, and R.W. Aldrich. 2000a. Cloning and functional characterization of novel potassium channel β subunits, hKCNMB3 and hKCNMB4. *J. Biol. Chem.* 275:6453–6461.

Brenner, R., G.J. Perez, A.D. Bonev, D.M. Eckman, J.C. Kosek, S.W. Wiler, A.J. Patterson, M.T. Nelson, and R.W. Aldrich. 2000b. Vasoregulation by the β1 subunit of the calcium-activated potassium channel. *Nature.* 407:870–876.

Butler, A., S. Tsunoda, D.P. McCobb, A. Wei, and L. Salkoff. 1993. mSlo, a complex mouse gene encoding "maxi" calcium-activated potassium channels. *Science.* 261:221–224.

Cox, D.H., and R.W. Aldrich. 2000. Role of the β1 subunit in large-conductance Ca^{2+}-activated K^+ channel gating energetics. Mechanisms of enhanced Ca^{2+} sensitivity. *J. Gen. Physiol.* 116:411–432.

Cox, D.H., J. Cui, and R.W. Aldrich. 1997a. Allosteric gating of a large conductance Ca-activated K^+ channel. *J. Gen. Physiol.* 110: 257–281.

Cox, D.H., J. Cui, and R.W. Aldrich. 1997b. Separation of gating properties from permeation and block in mslo large conductance Ca-activated K^+ channels. *J. Gen. Physiol.* 109:633–646.

Cui, J., and R.W. Aldrich. 2000. Allosteric linkage between voltage and Ca^{2+}-dependent activation of BK-type mslo1 K^+ channels. *Biochemistry.* 39:15612–15619.

Cui, J., D.H. Cox, and R.W. Aldrich. 1997. Intrinsic voltage dependence and Ca^{2+} regulation of *mslo* large conductance Ca-activated K^+ channels. *J. Gen. Physiol.* 109:647–673.

Diaz, L., P. Meera, J. Amigo, E. Stefani, O. Alvarez, L. Toro, and R. Latorre. 1998. Role of the S4 segment in a voltage-dependent calcium-sensitive potassium (hSlo) channel. *J. Biol. Chem.* 273: 32430–32436.

DiChiara, T.J., and P.H. Reinhart. 1995. Distinct effects of Ca^{2+} and voltage on the activation and deactivation of cloned Ca^{2+}-activated K^+ channels. *J. Physiol.* 489:403–418.

Gurnett, C.A., and K.P. Campbell. 1996. Transmembrane auxiliary subunits of voltage-dependent ion channels. *J. Biol. Chem.* 271: 27975–27978.

Ha, T.S., M.S. Heo, and C.S. Park. 2004. Functional effects of auxiliary β4-subunit on rat large-conductance Ca^{2+}-activated K^+ channel. *Biophys. J.* 86:2871–2882.

Hamill, O.P., A. Marty, E. Neher, B. Sakmann, and F.J. Sigworth. 1981. Improved patch-clamp techniques for high-resolution current recording from cells and cell-free membrane patches. *Pflugers Arch.* 391:85–100.

Horrigan, F.T., and R.W. Aldrich. 1999. Allosteric voltage gating of potassium channels II. Mslo channel gating charge movement in the absence of Ca^{2+}. *J. Gen. Physiol.* 114:305–336.

Horrigan, F.T., and R.W. Aldrich. 2002. Coupling between voltage sensor activation, Ca^{2+} binding and channel opening in large conductance (BK) potassium channels. *J. Gen. Physiol.* 120:267–305.

Horrigan, F.T., J. Cui, and R.W. Aldrich. 1999. Allosteric voltage gating of potassium channels I. Mslo ionic currents in the absence of Ca^{2+}. *J. Gen. Physiol.* 114:277–304.

Hu, L., J. Shi, Z. Ma, G. Krishnamoorthy, F. Sieling, G. Zhang, F.T. Horrigan, and J. Cui. 2003. Participation of the S4 voltage sensor in the Mg^{2+}-dependent activation of large conductance (BK) K^+ channels. *Proc. Natl. Acad. Sci. USA.* 100:10488–10493.

Isom, L.L., K.S. De Jongh, and W.A. Catterall. 1994. Auxiliary subunits of voltage-gated ion channels. *Neuron.* 12:1183–1194.

Knaus, H.G., K. Folander, M. Garcia-Calvo, M.L. Garcia, G.J. Kaczorowski, M. Smith, and R. Swanson. 1994a. Primary sequence and immunological characterization of β-subunit of high conductance Ca^{2+}-activated K^+ channel from smooth muscle. *J. Biol. Chem.* 269:17274–17278.

Knaus, H.G., M. Garcia-Calvo, G.J. Kaczorowski, and M.L. Garcia. 1994b. Subunit composition of the high conductance calcium-activated potassium channel from smooth muscle, a representative of the mSlo and slowpoke family of potassium channels. *J. Biol. Chem.* 269:3921–3924.

McManus, O.B., L.M. Helms, L. Pallanck, B. Ganetzky, R. Swanson, and R.J. Leonard. 1995. Functional role of the β subunit of high conductance calcium-activated potassium channels. *Neuron.* 14: 645–650.

Meera, P., M. Wallner, Z. Jiang, and L. Toro. 1996. A calcium switch for the functional coupling between α (hslo) and β subunits (KV,Ca β) of maxi K channels. *FEBS Lett.* 382:84–88.

Meera, P., M. Wallner, and L. Toro. 2000. A neuronal β subunit (KCNMB4) makes the large conductance, voltage- and Ca^{2+}-activated K^+ channel resistant to charybdotoxin and iberiotoxin. *Proc. Natl. Acad. Sci. USA.* 97:5562–5567.

Meredith, A.L., K.S. Thorneloe, M.E. Werner, M.T. Nelson, and R.W. Aldrich. 2004. Overactive bladder and incontinence in the absence of the BK large conductance Ca^{2+}-activated K^+ channel. *J. Biol. Chem.* 279:36746–36752.

Morales, S., P.J. Camello, G.M. Mawe, and M.J. Pozo. 2004. Cyclic AMP-mediated inhibition of gallbladder contractility: role of K^+ channel activation and Ca^{2+} signaling. *Br. J. Pharmacol.* 143:994–1005.

Nelson, M.T., and J.M. Quayle. 1995. Physiological roles and properties of potassium channels in arterial smooth muscle. *Am. J. Physiol.* 268:C799–C822.

Nimigean, C.M., and K.L. Magleby. 1999. β Subunits increase the calcium sensitivity of mSlo by stabilizing bursting kinetics. *Biophys. J.* 76:A328.

Nimigean, C.M., and K.L. Magleby. 2000. Functional coupling of the β1 subunit to the large conductance Ca^{2+}-activated K^+ channel in the absence of Ca^{2+}. Increased Ca^{2+} sensitivity from a Ca^{2+}-independent mechanism. *J. Gen. Physiol.* 115:719–736.

Niu, X., and K.L. Magleby. 2002. Stepwise contribution of each subunit to the cooperative activation of BK channels by Ca^{2+}. *Proc. Natl. Acad. Sci. USA.* 99:11441–11446.

Orio, P., and R. Latorre. 2005. Differential effects of β1 and β2 subunits on BK channel activity. *J. Gen. Physiol.* 125:395–411.

Qian, X., C.M. Nimigean, X. Niu, B.L. Moss, and K.L. Magleby. 2002. Slo1 tail domains, but not the Ca^{2+} bowl, are required for the β1 subunit to increase the apparent Ca^{2+} sensitivity of BK channels. *J. Gen. Physiol.* 120:829–843.

Rothberg, B.S., and K.L. Magleby. 2000. Voltage and Ca^{2+} activation of single large-conductance Ca^{2+}-activated K^+ channels described by a two-tiered allosteric gating mechanism. *J. Gen. Physiol.* 116:75–99.

Schreiber, M., and L. Salkoff. 1997. A novel calcium-sensing domain in the BK channel. *Biophys. J.* 73:1355–1363.

Shen, K.Z., A. Lagrutta, N.W. Davies, N.B. Standen, J.P. Adelman, and R.A. North. 1994. Tetraethylammonium block of Slowpoke calcium-activated potassium channels expressed in *Xenopus* oocytes: evidence for tetrameric channel formation. *Pflugers Arch.* 426:440–445.

Snetkov, V.A., and J.P. Ward. 1999. Ion currents in smooth muscle cells from human small bronchioles: presence of an inward rectifier K^+ current and three types of large conductance K^+ channel. *Exp. Physiol.* 84:835–846.

Stefani, E., M. Ottolia, F. Noceti, R. Olcese, M. Wallner, R. Latorre, and L. Toro. 1997. Voltage-controlled gating in a large conductance Ca^{2+}-sensitive K^+ channel (hslo). *Proc. Natl. Acad. Sci. USA.* 94:5427–5431.

Tanaka, Y., P. Meera, M. Song, H.G. Knaus, and L. Toro. 1997. Molecular constituents of maxi KCa channels in human coronary smooth muscle: predominant α + β subunit complexes. *J. Physiol.* 502:545–557.

Uebele, V.N., A. Lagrutta, T. Wade, D.J. Figueroa, Y. Liu, E. McKenna, C.P. Austin, P.B. Bennett, and R. Swanson. 2000. Cloning and functional expression of two families of β-subunits of the large conductance calcium-activated K^+ channel. *J. Biol. Chem.* 275:23211–23218.

Wallner, M., P. Meera, M. Ottolia, G.J. Kaczorowski, R. Latorre, M.L. Garcia, E. Stefani, and L. Toro. 1995. Characterization of and modulation by a β-subunit of a human maxi KCa channel cloned from myometrium. *Receptors Channels.* 3:185–199.

Wallner, M., P. Meera, and L. Toro. 1999. Molecular basis of fast inactivation in voltage and Ca^{2+}-activated K^+ channels: a transmembrane beta-subunit homolog. *Proc. Natl. Acad. Sci. USA.* 96: 4137–4142.

Wang, Y.W., J.P. Ding, X.M. Xia, and C.J. Lingle. 2002. Consequences of the stoichiometry of Slo1 α and auxiliary β subunits on functional properties of large-conductance Ca^{2+}-activated K^+ channels. *J. Neurosci.* 22:1550–1561.

Weiger, T.M., M.H. Holmqvist, I.B. Levitan, F.T. Clark, S. Sprague, W.J. Huang, P. Ge, C. Wang, D. Lawson, M.E. Jurman, et al. 2000. A novel nervous system β subunit that downregulates human large conductance calcium-dependent potassium channels. *J. Neurosci.* 20:3563–3570.

Xia, X.M., J.P. Ding, and C.J. Lingle. 1999. Molecular basis for the inactivation of Ca^{2+}- and voltage-dependent BK channels in adrenal chromaffin cells and rat insulinoma tumor cells. *J. Neurosci.* 19:5255–5264.

Xia, X.M., J.P. Ding, X.H. Zeng, K.L. Duan, and C.J. Lingle. 2000. Rectification and rapid activation at low Ca^{2+} of Ca^{2+}-activated, voltage-dependent BK currents: consequences of rapid inactivation by a novel β subunit. *J. Neurosci.* 20:4890–4903.

Xia, X.M., X. Zeng, and C.J. Lingle. 2002. Multiple regulatory sites in large-conductance calcium-activated potassium channels. *Nature.* 418:880–884.

Xu, J., W. Yu, J.M. Wright, R.W. Raab, and M. Li. 1998. Distinct functional stoichiometry of potassium channel β subunits. *Proc. Natl. Acad. Sci. USA.* 95:1846–1851.

Zeng, X.H., X.M. Xia, and C.J. Lingle. 2003. Redox-sensitive extracellular gates formed by auxiliary β subunits of calcium-activated potassium channels. *Nat. Struct. Biol.* 10:448–454.

Zhang, X., C.R. Solaro, and C.J. Lingle. 2001. Allosteric regulation of BK channel gating by Ca^{2+} and Mg^{2+} through a nonselective, low affinity divalent cation site. *J. Gen. Physiol.* 118:607–636.